Norwegian University
of Life Sciences

Master's Thesis 2023 60 ECTS
Faculty of Chemistry, Biotechnology and Food Science

Competitive patterns among strains of *Streptococcus pneumoniae* on plate and in broth

Karoline Stubmo
MSc Biotechnology

Competitive patterns among strains of *Streptococcus pneumoniae* on plate and in broth

Norwegian University of Life Sciences (NMBU),
Faculty of Chemistry, Biotechnology and Food Science

Acknowledgements

This thesis was conducted at the Faculty of Chemistry, Biotechnology and Food Science at the Norwegian University of Life Sciences under the supervision of Professor Knut Rudi and PhD Ida Ormaasen.

First, I would like to thank my main supervisor Knut Rudi. I am deeply thankful for the opportunity to conduct this thesis under your supervision. Your enthusiasm and creative thinking within the field have inspired me throughout this whole process.

Next, I would like to thank my co-supervisor and PhD Ida Ormaasen for always answering my questions with positivity. You have been a great support both regarding laboratory work, but also with data interpretation and the writing of this thesis.

Further, I would like to thank Postdoc Sara Arbulu Ruiz for providing me with so much of your time regarding all the laboratory work conducted at MolMik, but also throughout the writing process.

Also, I would like to thank Professor Morten Kjos for providing me with material and information during this research, and for showing interest in my results.

Furthermore, I would also like to thank both Laboratory Engineer Inga Leena Angell and Postdoc Morten Nilsen for your guidance in the laboratory and for always being so helpful and supportive. Thanks also to the rest of the MiDiv group for including me and making me feel welcome throughout this year.

Finally, a big thanks to my family and friends who have supported me throughout this year, especially my boyfriend Stian Heivand for always believing in me.

Ås, August 2023
Karoline Stubmo

Abstract

The human gut microbiota plays an important role in shaping the health of its host. Already during infancy, numerous bacterial species colonize the gut and social interactions among them influence the bacterial composition. A recent discovery revealed a correlation between strain diversity and genes encoding specific bacteriocins within the human infant gut. Thereby, this thesis aimed to investigate mechanisms that could potentially explain the high strain diversity of *S. pneumoniae* within the infant gut.

The study of this thesis involved investigation of competitive patterns among eight strains of *S. pneumoniae*. First, this involved intraspecific competition on agar plates, conducting overlay assays, to observe competitive outcomes in an environment similar to mucosal surfaces. Inhibition zones generated by producer strains were measured in overlay strains and average size of zones generated by each producer strain were calculated and compared. Further, three out of eight strains were selected for intraspecific competition in liquid broth to observe competitive outcomes in an environment similar to the gut lumen. Strains were mixed pairwise yielding different combinations of the same strains regarding initial culturing on blood- and yeast-enriched agar media. Samples of mixed cultures were taken 0, 3, and 5 hours into the competition and DNA extraction followed by Sanger sequencing was conducted to obtain interpretable results. Multilocus sequence typing was used to differentiate between strains in mixed cultures and a scoring system was created to calculate an approximate relative abundance of strains in mixed cultures at the different sampling points during competition. Mean relative abundance of strains in samples composed of the same strains were calculated and compared.

In conclusion, the results of the competition experiments indicate that reproductive strategies is a mechanism that could potentially explain the high strain diversity of *S. pneumoniae* within the infant gut. The two competition experiments yielded different competitive outcomes for the different strains regarding type of media. During competition on plate, Hermans-33 showed notable greater inhibitory capabilities compared to all the other strains, whereas when mixed with D39 and PMEN-14 during competition in broth, it was easily surpassed. These results aligns with the r/K selection theory implying D39 and PMEN-14 are r-strategists, exhibiting rapid growth, while Hermans-33 is a K-strategist, exhibiting competitive capabilities.

Sammendrag

Den menneskelige tarmmikrobiotaen spiller en viktig rolle i å forme vertens helse. Allerede i spedbarnsfasen koloniseres tarmen av mange bakteriearter, og sosiale interaksjoner mellom dem påvirker bakteriesammensetningen. En nylig oppdagelse har avdekket en sammenheng mellom stammediversitet og gener som koder for spesifikke bakteriosiner i tarmen til spedbarn. Dermed hadde denne oppgaven som mål å undersøke mekanismer som mulig kunne forklare den høye stammediversiteten av *S. pneumoniae* i spedbarnstarmen.

Studien i denne oppgaven involverte undersøkelse av konkurransemønstre blant åtte stammer av *S. pneumoniae*. Dette innebar først intraspesifikk konkurranse på agarskåler ved å gjennomføre overleggprøver for å observere konkurranseutfall i et miljø som er likt slimhinneoverflater. Hemmingssoner skapt av produsentstammer ble målt i overleggstammer, og gjennomsnittsstørrelsen på sonene skapt av hver produsentstamme ble beregnet og sammenlignet. Videre ble tre av åtte stammer valgt for intraspesifikk konkurranse i flytende medium for å observere konkurranseutfall i et miljø som er mer lik tarmens lumen. Stammene ble blandet parvis i ulike kombinasjoner med hensyn til initial dyrking på blod- og gjæranrikede agarskåler. Prøver fra blandingskulturer ble tatt 0, 3 og 5 timer inn i konkurransen, etterfulgt av DNA ekstraksjon og Sanger sekvensering for å oppnå tolkbare resultater. Multilokussekvenstyping ble brukt for å skille mellom stammer i blandingskulturer, og et skåringssystem ble opprettet for å beregne en omtrentlig relativ forekomst av stammer i blandingskulturer ved de ulike prøvetakingstidspunktene under konkurransen. Gjennomsnittlig relativ forekomst av stammer i blandingskulturer bestående av samme stammer ble beregnet og sammenlignet.

Konklusjonen er at resultatene fra konkurranseeksperimentene indikerer at reproduktive strategier mulig kan forklare den høye stammediversiteten av *S. pneumoniae* i spedbarnstarmen. De to konkurranseeksperimentene ga ulike konkurranseutfall for de ulike stammene med hensyn til type medium. Under konkurransen på skål viste Hermans-33 betydelig større hemmende evner sammenlignet med alle de andre stammene, mens den ble lett utkonkurrert av D39 og PMEN-14 under konkurransen i flytende medium. Disse resultatene samsvarer med r/K-seleksjonsteorien, ved anta at D39 og PMEN-14 er r-strateger med hurtig vekst, mens Hermans-33 er en K-strateg med konkurransedyktige egenskaper.

Abbreviations

A	Adenine
BLAST	The Basic Local Alignment Sequence Tool
bp	base pairs
C	Cytosine
DNA	Deoxyribonucleic acid
G	Guanine
GI	Gastrointestinal tract
MLST	Multilocus sequence typing
MSA	Multiple sequence alignment
N/A	Not applicable
O/N	Overnight
OD_{600}	Optical density at 600 nm
PBS	Phosphate-buffered saline
PCR	Polymerase chain reaction
PTM	Post-transitional modifications
QS	Quorum sensing
RNA	Ribonucleic acid
S.T.A.R.	Stool Transfer and Recovery
SNP	Single nucleotide polymorphism
T	Thymine
TAE	Tris-acetate EDTA
THY	Todd-Hewitt broth with yeast extract
TSA	Tryptic soy agar
TSA+SB	Tryptic soy agar with sheep blood
URT	Upper respiratory tract
WT	Wild type

Table of Contents

1 INTRODUCTION 1

1.1 The human infant gut 1
1.1.1 Development and ecological interactions of the gut microbiota 2

1.2 Structure and function of the gastrointestinal tract 4

1.3 Ecological reproductive strategies 5

1.4 The genus *Streptococcus* 6
1.4.1 *Streptococcus pneumoniae* 7

1.5 Technological approaches to study bacterial composition 9
1.5.1 DNA extraction 9
1.5.2 Polymerase chain reaction 9
1.5.3 Sequencing methods 9
1.5.4 Established methods to study bacterial competition 10

1.6 Aim of thesis 11

2 MATERIALS AND METHODS 12

2.1 General information of the materials and methods 12

2.2 Culturing and growth of *S. pneumoniae* strains 14
2.2.1 Preparation of growth media 14
2.2.2 Growth on plate 14
2.2.3 Growth in broth 14
2.2.4 Preparation of glycerol stocks 14
2.2.5 Growth curves 15
2.2.6 Microscopy 15

2.3 DNA extraction 16
2.3.1 Mechanical lysis of bacterial cells 16
2.3.2 Chemical lysis and magnetic separation of nucleic acids 16

2.4 Polymerase chain reactions 17
2.4.1 Primers and programs 17
2.4.2 Purification of PCR product 17

2.5 DNA quantification, qualification, and sequencing 19
2.5.1 Qubit quantification 19
2.5.2 Gel electrophoresis 19
2.5.3 Sanger sequencing 19

2.6 Competition on plate 20
2.6.1 Preparation of producer strain 20
2.6.2 Preparation of overlay strain 20
2.6.3 Overlay assay 20

2.7 Competition in broth 21
2.7.1 Growth of pure cultures 21
2.7.2 Normalization and preparation of mixed cultures 21
2.7.3 Sampling and growth curves 22

2.8 Data analysis 24
2.8.1 Strain selection and characterization 24
2.8.2 Statistical analysis of inhibitory effect during competition on plate 24
2.8.3 Calculating relative abundance of strains during competition in broth 25

3 RESULTS 27

3.1 Strain selection and characterization 27
3.1.1 16S sequencing 27
3.1.2 Multiple sequence typing 27
3.1.3 Growth curves 28
3.1.4 Microscopy 30

3.2 Competition experiments 31
3.2.1 Competition on plate 31
3.2.2 Competition in broth 35

4 DISCUSSION 38

4.1 *S. pneumoniae* strains exhibit varying competitiveness in diverse media 38
4.1.1 Strain diversity could potentially be explained by r/K selection theory 38
4.1.2 Previous research on intraspecific competition within S. pneumoniae 39

4.2 Type of agar medium influenced the competitive outcome 41
4.2.1 Blood stimulated greater inhibition than yeast 41
4.2.2 Strains cultured on same type of agar media expressed higher growth in broth 41

4.3 Growth curves unveils behavioral variations 42
4.3.1 Comparison of growth curves of pure cultures 42
4.3.2 Pure cultures exhibited higher growth rate than mixed cultures 42
4.3.3 Previous research on growth curves of mixed cultures 42

4.4 Methodological considerations of this research 43
4.4.1 *S. pneumoniae* is not a typical gut bacterium 43
4.4.2 Conflicting considerations regarding selection of competing strains 43
4.4.3 The scoring system of Sanger sequences was not an accurate approach 44
4.4.4 Limitations regarding quantification during experiments 44
4.4.5 Laboratory environments do not equal *in vivo* conditions 44

5 CONCLUSION 45

References 46

Appendices 50

Appendix A: Growth media 50
Appendix B: Gel electrophoresis 51
Appendix C: Polymorphic sites in gdh 54
Appendix D: Hemolysis on TSA+SB plates 55
Appendix E: Overlay assays after competition on plate 56
Appendix F: Relative abundance of strains during competition in broth 59

1 INTRODUCTION

The human body comprises a habitat for trillions of microorganisms which reach their highest densities within the gastrointestinal (GI) tract. Within the gut, a complex community, encompassing microbial populations, develops and is defined as the gut microbiota. Members of the gut microbiota belong to the three domains of life, including *Archaea*, *Bacteria*, and *Eukarya*. The human gut represents a dynamic ecosystem involved in a diverse set of interactions between the host and the microbes. These interactions are crucial for the development of the human immune system and thereby affecting the health of the host throughout life. Additionally, the gut microbiota contribute to the digestion food, liberating vital metabolites and vitamins, as well as protecting the host from colonization of pathogens. Fluctuations in the bacterial composition of the gut can harm the host by disrupting the continuous dialogue between the commensal bacteria within the intestines and the mucosal surfaces of their host (Milani et al., 2017). The composition of the microbiota is among other factors influenced by interactions among the bacterial species themselves. Within the human gut, bacteria are constantly fighting over space, nutrients, and other resources. In their fight to survive, many bacteria are producing antimicrobial peptides, called bacteriocins (Heilbronner et al., 2021). A recent study discovered a pattern where strain diversity of several species was associated with the presence of bacteriocins in the infant human gut (Ormaasen et al., 2023).

1.1 The human infant gut

The human infant gut is initially dominated by *Lactobacillus* and *Bifidobacterium*, which can promote the development of infant-acquired immunity and innate immunity (Yao et al., 2021). Given this symbiotic relationship between the gut bacteria and the host, the infant gut microbiota plays an important role in influencing the future health of its host. Alterations in the bacterial composition of the infant gut microbiota have been linked to pediatric disorders and other diseases further in life (Milani et al., 2017).

1.1.1 Development and ecological interactions of the gut microbiota

The establishment of the gut microbiota is believed to start immediately upon birth, while some studies even suggest it starts during gestation. Numerous factors are affecting the bacterial composition of the human infant gut, including gestational age, mode of delivery, feeding practices, antibiotic usage, maternal diet, and additional variables (Milani et al., 2017).

During vaginal birth, infants are exposed to the bacteria present in the vaginal and fecal microbiota of their mothers and fecal samples from these infants exhibit resemblances to the maternal vaginal flora. Consequently, vaginally delivered infants are commonly colonized by vagina-associated bacteria, such as *Lactobacillus* and *Prevotella* On the other hand, infants delivered by Caesarean section will not be exposed to the same type of bacteria and fecal samples of these infants rather exhibit resemblances to skin microbiota. Children born via Caesarean section are also more prone to colonization of microorganisms from hospital staff and the hospital environment (Avershina et al., 2016; Milani et al., 2017). Overall, vaginally delivered infants display higher levels of the proinflammatory *Bifidobacterium* and lower levels of the potential pathogenic *Enterococcus* and *Klebsiella* species than those delivered through Caesarean section (Reyman et al., 2019). An early establishment of *Bifidobacterium* and *Collinsella* as opposed to *Enterobacteriaceae* and *Streptococcus* during the initial six months of life is associated with extended gestation, vaginal childbirth, and adiposity at 18 months (Dogra et al., 2015).

Breastfeeding provides infants with optimal nourishment due to its essential nutrients and has been linked to increased levels of *Bifidobacterium* species. Although a high diversity within the adult gut microbiota is associated with good health, breastfed infants often exhibit lower diversity in their gut microbiota. This is thought to stem from the inhibitory effects of *Bifidobacteria* towards opportunistic pathogens (Differding & Mueller, 2020). Apart from its nutritional benefits, breastfeeding also contribute to the colonization of infant gut through bacterial transfer from the mother's skin and the infant's mouth (Biagi et al., 2018). During infancy, gut microbiota is characterized by low diversity which gradually expands throughout early development. In the early stages of life, the GI tract is predominantly populated by aerobic bacteria, whereas in adulthood these are mostly substituted by anaerobic bacteria. Upon introduction to solid foods, the gut microbiota begins resembling that of adults, and within three years they are hard to distinguish (Yao et al., 2021).

Over the course of evolution, bacteria have acquired the capacity to generate competitive agents for outcompeting or protecting themselves from other bacterial species. These antimicrobial substances are called bacteriocins and are ribosomally synthesized peptides, some of which undergo posttranslational modification (PTM) (Alvarez-Sieiro et al., 2016). Bacteriocins display high structural diversity and are encoded by complex and variable biosynthetic gene clusters that undergo rapid evolution and frequent horizontal gene transfer, a process involving the exchange of genetic material among bacteria (Heilbronner et al., 2021). Based on their structural difference, bacteriocins are categorized into three different classes. Class I bacteriocins encompass ribosomally synthesized peptides with PTM and a molecular weight less than 10 kDa. In contrast, class II bacteriocins consist of unmodified linear peptides also less than 10 kDa. Lastly, class III bacteriocins are unmodified bacteriocins exceeding 10 kDa, often composed of multiple domains and characterized by bacteriolytic or non-lytic properties (Alvarez-Sieiro et al., 2016).

Production of bacteriocins imposes a substantial physiological cost on bacteria and is primarily activated during competitive settings, regulated by producer cell densities sufficient to result in inhibitory concentrations (Heilbronner et al., 2021). This bacterial cell-to-cell signaling mechanism is called quorum sensing (QS) and relies and the autoinduction by small peptides, ultimately leading to gene expression (Reading & Sperandio, 2006). While certain bacteriocins exhibit specificity against closely related members of the same species or genera to the producer cell, others possess a wider range of activity, impacting unrelated bacterial strains. Bacteriocin production plays an important role in shaping microbial communities, either through facilitating or preventing the invasion of new bacterial strains or by redistributing the community members into sub-niches (Heilbronner et al., 2021).

1.2 Structure and function of the gastrointestinal tract

The GI tract constitutes a vital organ system responsible for food digestion, nutrient absorption, enzyme and water secretion, and waste excretion. It encompasses the oral cavity, pharynx, esophagus, stomach, small intestine, large intestine, and the anal canal. Additionally, it includes accessory structures such as the teeth, tongue, salivary glands, liver, gallbladder, and pancreas (Ogobuiro et al., 2023; Tobias & Sadiq, 2023). The primary role of the small intestine, also called ileum, is the absorption of nutrients and minerals from food, while the colon, including the large intestine and the anal canal, is responsible for extraction of water and salt from solid waste materials (Mann et al., 2016).

From the inside of the gut, called lumen, there are four distinct layers making up the GI tract. The initial layer, known as the mucosa, consist of a single layer of epithelium which is highly folded to increase its surface area and thereby its absorption potential. Within this layer are many invaginations forming tubular exocrine glands which secrete mucus, electrolytes, water, and digestive enzymes. Additionally, the mucosa contains endocrine glands which secrete hormones and is supported by a thin layer of connective tissue, called the lamina propria. The next layer, called the submucosa, is also a layer of connective tissue which contains blood and lymphatic vessels. The subsequent layer, called muscularis externa, comprises two layers of smooth muscle tissue responsible for moving the food through the GI tract. Lastly, the outermost layer is called the serosa and encompasses another layer of connective tissue alongside a delicate cellular layer which secrete lubricating fluids to reduce friction within internal structures (Ogobuiro et al., 2023).

Within the GI tract, a multitude of commensal bacteria and pathogens engage in a continuous communication with both each other and their human host. To prevent inflammation, dendritic cells, also called antigen-presenting cells, play a crucial role in maintaining a balance between immune responses against invading pathogens and tolerance of commensal bacteria. They achieve this by recognizing and responding to bacteria and their byproducts. Together with macrophages, they express pattern recognition receptors and communicate with the mesenteric lymph nodes and Peyer's Patches to determine a potential immune response (Mann et al., 2016).

1.3 Ecological reproductive strategies

In ecology, there are two distinct reproductive strategies, known as r-selection, where the *r* denotes intrinsic growth rate, and K-selection, where the *K* refers to the carrying capacity. The terminologies were introduced by MacArthur and Wilson in 1967, although the underlying theories were initially postulated by Dobzhansky in 1950, aiming to elucidate the mechanisms of natural selection in tropical regions as opposed to temperate zones (Pianka, 1970). The theory has been subject to criticism for not accounting for the life history of animals. Given the fact that bacteria reproduce through binary fission and lack a life history similar to more complex organisms, it has proven to apply well for microorganisms (Andrews & Harris, 1986).

The r/K selection theory suggests that selection pressure within an environment drives selection in one of two generalized directions, favoring species with different growth strategies. The r-selected species display rapid growth rates alongside limited competitive abilities, whereas the K-selected species exhibit traits advantageous in densely populated environments when resources are limited, particularly when the population approaches the environmental carrying capacity (Freilich et al., 2010; Vadstein et al., 2018). Bacterial species exhibiting r-selection are often labeled as opportunistic, and pathogens are frequently identified as r-strategists (Vadstein et al., 2018). Characteristic properties of both r- and K-strategists, and also pioneer and mature communities, is outlined in table 1.1.

Table 1.1: Characteristics of r/K-strategic species and of pioneer/mature communities. The table, borrowed from the article by Vadstein et al. from 2018, outlines the characteristic properties of r- and K-strategists and also pioneer and mature communities.

Species level:	**r-strategists**	**K-strategists**
Maximum growth rate	High	Low
Biomass at carrying capacity	Unstable	Stable
Effect of enrichment/instability	Rapid growth	Slow growth
Competitive ability at low substrate supply per capita	Poor	Good
Affinity to substrate	Low	High
Community level:	Pioneer	Mature
Biological control	Low	High
Stability to perturbations	Poor	Good
Diversity	Low	High
Niche width	Wide	Narrow
Specialization	Low	High

1.4 The genus *Streptococcus*

Streptococcus is a genus of Gram-positive, nonmotile, non-spore forming, and catalase-negative bacteria with a spherical or ovoid shape that are typically arranged in chains or pairs. The genus is named for their shape and structural organization, with the Latin word "streptos" meaning twisted and the word "coccus" meaning berries. Streptococci colonize human and animal mucous membranes, which makes them part of the physiological flora in the oral cavity, the upper respiratory tract (URT), and the GI tract. Certain species within the *Streptococcus* genus are part of the core microbiota of the infant gut and can be detected within the first 24 hours following birth. Typically, they occur as opportunistic pathogens, causing disease primarily during weak immunological response within its host (Krzyściak et al., 2013; Milani et al., 2017).

Most streptococci are facultative anaerobes, while some are obligate anaerobes. They have complex nutritional requirements, and most of them require blood-enriched media (Hardie & Whiley, 1995; Patterson, 1996). Streptococci can be classified into three groups based on their hemolytic effect displayed on blood agar, with β-hemolytic streptococci performing complete lysis of red blood cells giving clear zones on the agar, α-hemolytic streptococci performing partial hemolysis giving green zones on the agar, and γ-hemolytic streptococci having no hemolytic effect. The hemolytic effect of streptococci is affected by age of red blood cells as well as species, with some species performing several types, thereby this classification is not completely satisfactory. Instead, classification based on serologic specificity, which involves their antigenic differences in cell wall carbohydrates, is the standard (Patterson, 1996). This classification groups streptococci into groups A-V, with group A *Streptococcus* (GAS), including species *S. pneumoniae* and *S. pyogenes*, and group B *Streptococcus* (GBS), including *S. agalactiae*, causing the most common infections. In total, the genus of *Streptococci* is one of the most invasive groups of bacteria, divided into 49 species and eight subspecies (Krzyściak et al., 2013).

1.4.1 *Streptococcus pneumoniae*

Streptococcus pneumoniae, also called "pneumococcus", is a Gram-positive, opportunistic human pathogen, causing both invasive and non-invasive infections globally. It particularly affects children, elderly, and individuals with weakened immune systems (Kjos et al., 2016). The pathogen has the potential to induce severe illnesses such as community-acquired pneumonia, meningitis, otitis media, and sepsis. However, it often persists asymptomatically in healthy individuals after colonization during childhood. Commensal carriage is a normal occurrence, with rates ranging from 20-50 % in children and 5-20 % in adults in more developed countries. In contrast, rates can reach as high as 90 % in children and 50 % in adults in less developed countries. Notably, colonization with multiple strains is widespread, and competition between different strains within the host is believed to be an important factor influencing pneumococcal diversity and disease progression (Kjos et al., 2016; Miller et al., 2018).

Pneumococci colonize mucosal surfaces of the human body, specifically the URT (Weiser et al., 2018). These bacteria typically grows in the human nasopharynx as spatially structured colonies or biofilm, which is highly structured communities of cells producing an extracellular matrix to help them adhere to surfaces. These biofilms protect the pathogen from both host immune responses and antimicrobial agents, contributing to their resilience and survival (Chao et al., 2014; Weiser et al., 2018).

Invasive infections are caused by the bacteria being infiltrated into the mucosal surface on top of epithelial cells within the human nasopharynx. From here, the pneumococci can spread to the middle ear, lungs, brain, and blood. If they enter the blood, they also gains access to the central nervous system, the heart, and the spleen. In such tissues, they will be exposed to attacks by the immune system and also encounter diverse environmental conditions than what they have in the nasopharynx (Aggarwal et al., 2020). Pneumococci has been detected in the human infant gut and are assumed to enter the GI tract through contamination while nursing following the swallowing of breastmilk (Biagi et al., 2018).

Similar to other bacterial pathogens, pneumococci are coated by a polysaccharide capsule crucial for its virulence. In total, strains of *S. pneumoniae* produce one out of 90 different polysaccharide capsules which are believed to have evolved as a mechanism to evade the human immune system (Bentley et al., 2006). The capsule of *S. pneumoniae* is hyaluronic, which provide resistance to phagocytosis, enabling the bacteria to evade a key defense mechanism within its host and spread to multiple organs (Patterson, 1996).

The species of *S. pneumoniae* is known to have at least four different bacteriocin systems. One of them is bacteriocin-like peptides (Blp), encoded by the *blp* operon (Miller et al., 2016). Blp produced by pneumococci, also called "pneumocins", are antimicrobial peptides similar to bacteriocins. The *blp* locus is ubiquitous in the genome of pneumococcal strains and organized in biosynthetic gene clusters comprised of several operons, with expression regulated by a QS system (Kjos et al., 2016).

1.5 Technological approaches to study bacterial composition

1.5.1 DNA extraction

DNA extraction is a method to isolate deoxyribonucleic acid (DNA) utilizing physical and chemical techniques to separate DNA from cell membranes, proteins, and other cellular components (Gupta, 2019). The first successful isolation of DNA was conducted by the Swiss physician Friedrich Miescher in 1869 during his attempt to isolate cells from lymph nodes (Tan & Yiap, 2009). Extraction of DNA is initiated by physically lysing cells and thereby releasing the nucleic acids within them, followed by chemical or enzymatical methods to remove macromolecules, lipids, ribonucleic acids (RNA), and proteins (Gupta, 2019).

1.5.2 Polymerase chain reaction

Polymerase chain reaction (PCR) is an amplification technique that involves denaturation and renaturation of short DNA segments, utilizing Taq polymerase, a DNA polymerase isolated from *Thermus aquaticus*. This method was introduced by Mullis and his colleagues in 1985, leading to their Nobel prize recognition (Khehra et al., 2023). The process utilizes a thermocycler to amplify specific DNA segments through a series of three steps. In the first step, double-stranded DNA (dsDNA) is denatured at high temperatures ranging from 92-95°C. Subsequently, during the second step, primers specific to the target DNA segment are annealed at 50-70°C. Finally, the third step facilitates the extension of the dsDNA molecules at 72°C. All steps are repeated for 30-40 cycles, depending on the desired amount of DNA (Gupta, 2019).

1.5.3 Sequencing methods

Sanger sequencing is a method of DNA sequencing developed by Frederick Sanger in 1977. This method involves determination of the nucleotide sequence in single-stranded DNA molecules through complementary synthesis of polynucleotide chains and the selective integration of fluorescently labeled chain-terminating dideoxynucleotides, ultimately performed by DNA polymerase I (Sanger et al., 1977; Totomoch-Serra et al., 2017). For more than three decades, this sequencing technique served as the standard method for genome sequencing and remains the predominant choice for sequencing short segments of DNA (Dewey et al., 2012).

The 16S rRNA gene has become the primary housekeeping gene employed as a genetic marker for investigating bacterial phylogeny and taxonomy (Janda & Abbott, 2007). The gene is about 1550 base pairs (bp) long and comprises both conserved and variable regions, including interspecific polymorphisms that provide unique and statistically significant measurements. The conserved regions of the gene are targeted by universal primers due to complementarity, whereas the variable regions are used for comparative taxonomy (Clarridge, 2004).

Multilocus sequence typing (MLST) is a sequencing method where fragments of about 500 bp from housekeeping genes are sequenced to differentiate between different strains of the same species by identifying unique polymorphic sites within each strain. The method has proven effective in typing strains and examining the population structure of numerous human pathogens, including *Streptococcus pneumoniae* (Jones et al., 2003).

1.5.4 Established methods to study bacterial competition

One approach to study competitive activity among bacteria is to conduct an overlay assay where producer strains are stabbed into agar plates and incubated for a few hours, followed by an overlay strain being poured over the stabbed agar and further incubated. The producer strains stabbed into the agar might show inhibitory effect in the overlay strain, which will occur as clear zones around the stabbed strains and can be measured in diameter. Given that the overlay assay is a qualitative assay and inhibition can vary depending on the number of bacteria that was stabbed into the plate, quantitative assessments must be interpreted with caution (Maricic & Dawid, 2014).

Another approach to study competition among bacteria is the creation of a mixed population in a given model system where subsequent sampling of the population are conducted to analyze its dynamics during a period of time. The abundance of each bacterial strain in the mixed population at different sampling points can be quantified using a genetic marker to differentiate between strains considering polymorphic sites among strains. By sequencing samples of the mixed population, relative abundance of each strain can be calculated creating a model to interpret the variation in signals emitted for polymorphic sites and thereby quantify relative abundance of each bacterial strain. Partial least-squares regression is an example of a model that was proven effective for quantifying relative abundance of strains using the 16 rRNA gene as genetic marker (Trosvik et al., 2007).

1.6 Aim of thesis

A recent discovery indicated a positive correlation between the presence of genes encoding specific bacteriocins and strain diversity among different species of *Streptococcus*, including *S. salivarius*, *S. thermophilus*, and *S. pneumoniae*, in the human infant gut (Ormaasen et al., 2023). These findings raised questions regarding which mechanisms influence strain diversity within the infant gut microbiota.

The aim for this research was to investigate mechanisms that could potentially explain the high diversity of *S. pneumoniae* strains within the human infant gut. To investigate this, the following sub goals were set:

1. Characterize strains of *S. pneumoniae* regarding growth, morphology, and genetic variation
2. Investigate intraspecific pneumococcal competition on agar plate, creating an environment similar to mucosal surfaces
3. Investigate intraspecific pneumococcal competition in liquid broth, creating an environment similar to gut lumen

The rationale for selecting *S. pneumoniae* as the model organism in this research was driven by its role as a common model organism within the field of microbiology. Several methods, including the overlay assay conducted by Maricic & Dawid in 2014 and the assays conducted by Miller et al. in 2018, have been established to study intraspecific interactions among pneumococcal strains. The strains used in the study by Miller et al. were available for research and provided by Professor Morten Kjos who contributed equally with Miller.

2 MATERIALS AND METHODS

2.1 General information of the materials and methods

The research of this thesis involved experimental studies of a total of eight strains of *S. pneumoniae*, including the strains D39, FB145 , Hermans-33, MK1203, PMEN-2, PMEN-14, PMEN-18, and TIGR4. The strain D39 is a clinical isolate originally isolated in 1916 and has been a leading model for pneumococcal pathogenesis (Lanie et al., 2007). The strain FB145 is a recently transformed strain D39 lacking the native *blp* regulatory genes, *blpSRHC* (Miller et al., 2018). The strain MK1203 is another recently transformed strain D39 lacking the genes encoding CAAX proteases, which are putative immunity proteins against specific bacteriocins (Miller et al., 2016). The strain Hermans-33 is an isolated wild type (WT) of *S. pneumoniae*. Likewise, are strains PMEN-2, PMEN-14, and PMEN-18, which are all part of the Pneumococcal Molecular Epidemiology Network (PMEN) established in 1997 to standardize classification and create a global collection of resistant clones of pneumococci (Golden et al., 2018). Lastly, the WT strain TIGR4 is a specifically virulent strain of *S. pneumoniae* (Lanie et al., 2007).

The bacterial samples investigated in this research were supplied by the Molecular Microbiology (MolMik) research group at the faculty of Chemistry, Biotechnology, and Food Science (KBM) at the Norwegian University of Life Sciences (NMBU). All experimental research concerning viable bacteria was conducted in the MolMik laboratory, whereas experimental procedures involving non-viable bacteria for DNA extraction and subsequent analysis were carried out in the laboratory of the Microbial Diversity (MiDiv) research group, also at the faculty of KBM at NMBU. A flowchart of the research progress is illustrated in figure 2.1.

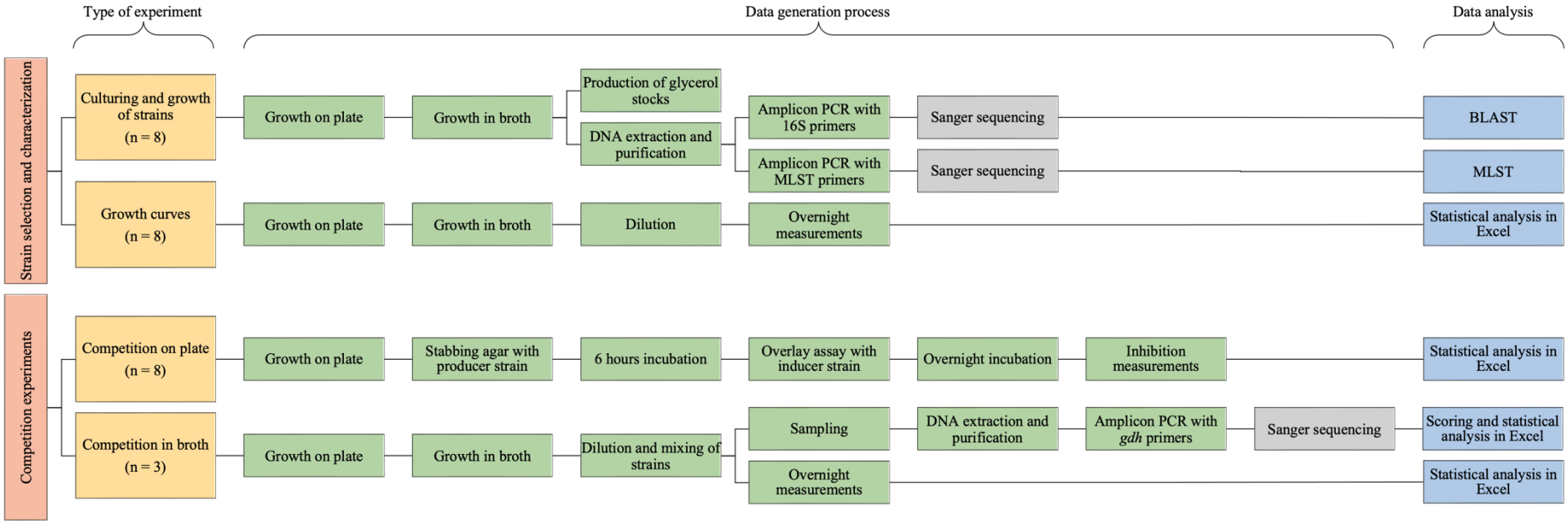

Figure 2.1: Flowchart of the research progress. The flowchart illustrates the progression of research in this thesis through a comprehensive flowchart. The research is divided into two distinct parts: strain selection and characterization, followed by competition experiments, both depicted by orange boxes. Each type of experiment is represented by yellow boxes, and green boxes provide detailed explanations of the data-generating processes involved in each experiment. The sequencing procedures carried out by Eurofins Genomics in Germany are denoted by grey boxes, while the data analysis conducted by the master student is indicated by blue boxes.

2.2 Culturing and growth of *S. pneumoniae* strains

2.2.1 Preparation of growth media

The experimental work for this thesis started by culturing and promoting the growth of the strains, necessitating the preparation of suitable media to support pneumococcal growth. Several types of media were used in the experiments, including Todd-Hewitt broth with Yeast extract (THY), THY agar, THY soft agar, Tryptic Soy Agar (TSA), and Tryptic Soy Agar with 5 % Sheep Blood (TSA+SB) (Thermo Fisher Scientific, USA). See appendix A for reagents used to prepare THY, THY agar, THY soft agar, and TSA.

2.2.2 Growth on plate

In preparation to each experiment, glycerol stocks of strains were streaked out on agar plates and incubated overnight (O/N) at 37°C under anaerobic conditions with 5 % CO_2, using a 3.5 L Anaerobic jar (Thermo Fisher Scientific, USA) in combination with the 3.5 L gas generating sacket AnaeroGen^{TM} (Thermo Fisher Scientific, USA).

2.2.3 Growth in broth

Isolated colonies on agar plates were transferred to sterile glass tubes containing 5 ml of THY and incubated in a water bath at 37°C. Optical density at 600 nm (OD_{600}) were measured consistently until 0.3-0.5, which indicates exponential growth, before transferred to further usage.

2.2.4 Preparation of glycerol stocks

Upon reaching exponential growth, 600 µl of cells in THY were transferred to sterile Eppendorf tubes (Eppendorf, Germany) and mixed with 400 µl of 50 % glycerol. This gave glycerol stocks with 80 % of bacteria combined with 20 % of glycerol, which were marked and kept in the freezer at -80°C for further usage throughout the research.

2.2.5 Growth curves

All strains were cultivated in THY until an OD_{600} of 0.3-0.5, before diluted to an OD_{600} of 0.05 by the addition of extra THY. Further, 300 µl of all strains were transferred to wells on a plate, as illustrated in figure 2.2, to be measured using the Synergy H1 Hybrid Reader (BioTek, USA) and the software Gen5 2.01 (BioTek, USA). Samples were measured at OD_{600} every ten minutes for 20 hours and shaken 5 seconds prior to every measurement. After 20 hours, the plate was discarded, and the data was exported to an Excel-file for further analysis.

H_2O	H_2O	H_2O	H_2O	H_2O	H_2O	H_2O	H_2O	H_2O	H_2O	H_2O	H_2O
H_2O	D39	FB	H33	MK	P2	P14	P18	T4	THY	THY	H_2O
H_2O	D39	FB	H33	MK	P2	P14	P18	T4	THY	THY	H_2O
H_2O	D39	FB	H33	MK	P2	P14	P18	T4	THY	THY	H_2O
H_2O	D39	FB	H33	MK	P2	P14	P18	T4	THY	THY	H_2O
H_2O	D39	FB	H33	MK	P2	P14	P18	T4	THY	THY	H_2O
H_2O	D39	FB	H33	MK	P2	P14	P18	T4	THY	THY	H_2O
H_2O	H_2O	H_2O	H_2O	H_2O	H_2O	H_2O	H_2O	H_2O	H_2O	H_2O	H_2O

Figure 2.2: Plate organization of pure cultures during growth measurements. The figure illustrates how the pure cultures of strains THY, depicted in orange, were organized to produce six replicates for growth measurements of each strain. Depicted in yellow, some wells were filled with THY to work as a blank control when measuring growth, while the outer wells were filled with distilled water (H_2O), depicted in blue, to prevent evaporation of samples.

2.2.6 Microscopy

In preparation, strains D39, Hermans-33, and PMEN-14 were incubated O/N on TSA at 37°C with 5 % CO_2. Sterile loops were used to slightly touch single colonies of each strain which were further diluted in PBS. A small drop of each diluted strain was placed on a layer of agarose on a glass plate and studied in the Zeiss LSM 700 microscopy.

2.3 DNA extraction

To extract DNA from the bacteria, a sufficient number of cells was required to get sufficient sequence quality. When strains were grown in THY broth and reached an OD^{600} of 0.3-0.5, samples of 1 ml were transferred to sterile 1.5 ml tubes. The samples were spun down using the Centrifuge 5424 (Eppendorf, Germany) at 6200 rpm for 1 minute until a pellet was formed at the bottom. Further, the supernatant was discarded, and the pellet was washed and dissolved in 1 ml of 1x PBS. Again, the samples was centrifuged to form a pellet and the supernatant was discarded. Lastly, the pellet was dissolved in 200 µl of Stool Transfer And Recovery (S.T.A.R.) Buffer (Roche, Switzerland) and placed in the freezer at -20°C for further usage.

2.3.1 Mechanical lysis of bacterial cells

The initial step of DNA extraction involved mechanical lysis of bacterial cells. To prepare, FastPrep-tubes (MP Biomedicals, USA) were filled with sterile glass beads of three different sizes: 0.2 g of beads with a diameter of 106 µm, 0.2 g of beads with a diameter of 600 µm, and 2 beads with a diameter of 2 mm. The bacterial samples were then added to the beads and subjected to centrifugation using the MagNa Lyser at 6200 rpm for 40 seconds, twice, with 5 minutes of rest between treatments.

2.3.2 Chemical lysis and magnetic separation of nucleic acids

Extraction of DNA was conducted using the mag midi kit (LGC, UK). The mag™ kits employs a magnetic separation technique for the extraction of nucleic acids utilizing superparamagnetic particles coated with a mag surface chemistry. This surface binds nucleic acids that are presented in samples before they are washed to remove excess substances and eluted to be used in further research. After extraction following the manufacturer's recommendations, template DNA was placed in the freezer at -20°C for further usage.

2.4 Polymerase chain reactions

2.4.1 Primers and programs

The primers used for MLST of *S. pneumoniae* strains targets internal fragments of seven housekeeping genes listed in table 2.1. These were ordered from Thermo Fisher Scientific and added nuclease-free water to a concentration of 100 μM. The primers used for 16S sequencing targets the gene encoding 16S rRNA in bacterial genomes, also listed in table 2.1. Ahead of PCR, primers were diluted 1:10 to a concentration of 10 μM.

The reaction mixture for amplifying the MLST genes and the 16S rRNA gene both comprised 1x HOT FIREPol® RTL (Solis BioDyne, Estonia), 0.2 μM of each primer, and nuclease-free water. Recommended amount of template DNA for amplification of the MLST genes was 0.1-10 ng, while it was 10-100 ng for the 16S rRNA gene.

Amplification of MLST genes was performed with 2720 Thermal Cycler (Applied Biosystem, USA) using a program starting with 15 minutes initial denaturation at 95°C followed by 25 cycles of denaturation at 95 °C for 30 seconds, annealing at 50°C for 30 seconds, and elongation at 72°C for 45 seconds. The program was completed by a final elongation at 72°C for 7 minutes before the plate was set at 10°C until further usage.

Amplification of the 16S rRNA gene was performed with the same machine using a program with 15 minutes initial denaturation at 95°C followed by 30 cycles of denaturation at 95 °C for 30 seconds, annealing at 55°C for 30 seconds, and elongation at 72°C for 1 minute and 20 seconds. Finally, the plate was set at 10°C until further usage.

2.4.2 Purification of PCR product

The PCR products were purified using paramagnetic selectively binding AMPure® XP beads (Beckman Coulter, USA) at a 1:1 ratio. These beads only binds DNA fragments of 100 bp or more, meaning that excess primers, nucleotides, salts, and enzymes will be removed through a washing procedure using 80 % ethanol following the manufacturer's recommendations.

Table 2.1: Primers utilized in PCR. Information about primers utilized in PCR during the research of this thesis.

Target gene	Primer name	Amplicon (bp)	Primer sequences F/R (5' to 3')	Primer length (bp)	GC (%)	Reference
aroE	aroE-up		GCC TTT GAG GCG ACA GC	17	65	
		479				(Jolley et al., 2018)
	aroE-dn		TGC AGT TCA RAA ACA TWT TCT AA	23	28	
gdh	gdh-up		ATG GAC AAA CCA GCN AGY TT	20	45	
		659				(Jolley et al., 2018)
	gdh-dn		GCT TGA GGT CCC ATR CTN CC	20	60	
gki	gki-up		GGC ATT GGA ATG GGA TCA CC	20	55	
		626				(Jolley et al., 2018)
	gki-dn		TCT CCC GCA GCT GAC AC	17	65	
recP	recP-up		GCC AAC TCA GGT CAT CCA GG	20	60	
		572				(Jolley et al., 2018)
	recP-dn		TGC AAC CGT AGC ATT GTA AC	20	45	
spi	spi-up		TTA TTC CTC CTG ATT CTG TC	20	40	
		560				(Jolley et al., 2018)
	spi-dn		GTG ATT GGC CAG AAG CGG AA	20	55	
xpt	xpt-up		TTA TTA GAA GAG CGC ATC CT	20	40	
		572				(Jolley et al., 2018)
	xpt-dn		AGA TCT GCC TCC TTA AAT AC	20	40	
ddl	ddl-up		TGC YCA AGT TCC TTA TGT GG	20	48	
		514				(Jolley et al., 2018)
	ddl-dn		CAC TGG GTR AAA CCW GGC AT	20	53	
16S rRNA	Mangala F-1		TCC TAC GGG AGG CAG CAG	18	67	
		1200				Genetic Analysis
	16S 1015U R		CGG TTA CCT TGT TAC GAC TT	20	45	

2.5 DNA quantification, qualification, and sequencing

2.5.1 Qubit quantification

Quantification of DNA was conducted utilizing the Qubit® dsDNA HS Assay Kit (Invitrogen, USA). This assay includes a dye that exhibits high selectivity for double-stranded DNA (dsDNA). Upon binding to dsDNA, the dye emits a fluorescence signal, detectable by a Qubit Fluorometer (Invitrogen, USA). Following the manufacturer's recommendations, 2 µl sample was mixed with 198 µl working solution.

2.5.2 Gel electrophoresis

DNA qualification was accomplished through gel electrophoresis using a 1 % agarose gel composed of UltraPure™ Agarose (Invitrogen, USA) and 1x tris-acetate EDTA (TAE) buffer. Agarose is a sugar compound of L- and D-galactose subunits, and when dissolved it creates a non-covalently bound network with molecular filtering properties. Before solidification in a gel chamber, the gel is added 4 µl PeqGREEN (Peqlab, Germany) for every 50 ml of gel, which binds DNA and emits fluorescence when exposed to UV light.

Before loading the gel, samples were added a loading dye providing weight to help them fall down into the wells of the gel. The color of the dye also makes it possible to see the negatively charged DNA strands migrate through the gel. The electrophoresis were run at 80 V and 400 mA for 35 minutes before the bands were visualized by UV light utilizing the Molecular Imager® Gel Doc™ XR Imaging System and the software Quantity One 1-D (BioRad, USA). A 100 bp DNA ladder (Solis BioDyne, Estonia) was loaded in the first well as a size marker.

2.5.3 Sanger sequencing

In accordance with guidelines provided by Eurofins Genomics, purified PCR products were individually mixed with forward and reverse primers at a concentration of 5 pmol/µl. This was done at a 1:1 ratio, resulting in a total volume of 10 µl in each tube. For amplicons ranging from 300 to 1000 bp, the recommended concentration was 5 ng/µl, and for amplicons of 1000 to 3000 bp, the recommended was 10 ng/µl. The samples were dispatched via mail and results were delivered online within 2-4 business days.

2.6 Competition on plate

The experimental procedure of competition on plate was inspired by the overlay assays outlined by Maricic & Dawid in 2014.

2.6.1 Preparation of producer strain

All strains were streaked out on TSA+SB plates and incubated O/N at 37°C with 5 % CO_2. Further, TSA plates were prepared by pipetting 4 000 units of catalase onto them and spreading it using a sterile glass bead, thereby removing the inhibitory effects of pneumococcal production hydrogen peroxide (H_2O_2). The plates were dried for about 10 minutes before a visible quantity of each strain was stabbed into their pre-designated spots on each TSA plate using sterile pipette tips for each stab. Lastly, the stabbed TSA plates were incubated at 37°C with 5 % CO_2 for 6 hours. After incubation the initial incubation of strains on the blood-enriched TSA+SB, the plates were examined for hemolysis.

2.6.2 Preparation of overlay strain

All strains were streaked out on THY agar plates and incubated O/N at 37°C with 5 % CO_2. Following incubation, 5-10 colonies of each strain were inoculated to 5 ml of THY broth and grown to mid-exponential phase in a 37°C water before used to make glycerol stocks.

2.6.3 Overlay assay

Glycerol stocks of strains grown to mid-exponential phase were thawed at room temperature and THY soft agar was melted in the microwave before 10 ml were transferred to sterile glass tubes and put in a water bath at 42°C to keep the agar from solidifying. Just prior to the overlay, 4 000 units of catalase and 400 µl of the glycerol stock was added before poured gently onto the stabbed and incubated TSA plates. It was important to compose the overlay mixture one by one to prevent the agar from solidifying and to it pour it gently onto the TSA plates to prevent the stabbed cultures being pulled into the overlay. After pouring, the overlay was let to solidify for 10 minutes before the plates were incubated O/N at 37°C with 5 % CO_2. Following incubation, plates were examined, and the diameter of transparent zones around the stabbed strains was measured in millimeter (mm), indicating the inhibition of the overlay strain. The competition on plate was conducted twice, with the second round only including producer strains cultured on TSA+SB.

2.7 Competition in broth

After characterizing the eight strains, three out of eight strains were chosen primarily based on genetic variation to further investigate their competitive patterns in liquid media. Consequently, the competition experiment in broth included the *S. pneumoniae* strains D39, Hermans-33 and PMEN-14.

2.7.1 Growth of pure cultures

The three strains were grown on both THY and TSA+SB plates to test if the type of media influenced the competitiveness of the strains. After O/N incubation, 5-10 colonies of each strain from each type of agar were transferred to 5 ml THY broth in sterile glass tubes which were then incubated in a water bath at 37°C. When reaching exponential growth phase between OD_{600} 0.3-0.5, the strains were put on ice for a short time period while calculating normalization.

2.7.2 Normalization and preparation of mixed cultures

When the strains were confirmed to grow exponentially, they were all normalized to an OD_{600} of 0.05, before mixed with each of the other strains, including those cultured on TSA+SB and THY plates, yielding a total of twelve different combinations of strains, as listed in table 2.2.

Table 2.2: Mixed cultures of strains. The table presents the twelve mixed cultures of strains D39, Hermans-33, and PMEN-14 cultured on THY and TSA+SB prepared for competition in broth.

Mixed culture	Strain 1, agar	Strain 2, agar
1	D39, TSA+SB	Hermans-33, TSA+SB
2	D39, TSA+SB	PMEN-14, TSA+SB
3	Hermans-33, TSA+SB	PMEN-14, TSA+SB
4	D39, TSA+SB	Hermans-33, THY
5	D39, TSA+SB	PMEN-14, THY
6	Hermans-33, TSA+SB	PMEN-14, THY
7	D39, THY	Hermans-33, THY
8	D39, THY	PMEN-14, THY
9	Hermans-33, THY	PMEN-14, THY
10	D39, THY	Hermans-33, TSA+SB
11	D39, THY	PMEN-14, TSA+SB
12	Hermans-33, THY	PMEN-14, TSA+SB

2.7.3 Sampling and growth curves

After mixing strains, 300 µl of each mixed culture was transferred to sterile 1.5 ml tubes and prepared for DNA extraction and further analysis. Further, 300 µl of each combination was added to five pre-designated wells on a plate for further growth and sampling, as illustrated in figure 2.3. The outer wells of the plate were filled with distilled water to prevent evaporation of the samples and THY broth as a blank control when measuring growth of the samples.

After correctly transferring all samples to the plate, the plate reader was started using the same program as when measuring growth curves of pure cultures. Both of the latter samplings was conducted by pausing the plate reader and carefully transferring 300 µl of each mixed culture to sterile 1.5 ml tubes for preparation to DNA extraction and further analysis.

	Sampled at 3 hours				Sampled at 5 hours				Growth curves		
H_2O	H_2O	H_2O	H_2O	H_2O	H_2O	H_2O	H_2O	H_2O	H_2O	H_2O	H_2O
H_2O	1	7	1	7	1	7	1	7	1	7	THY
H_2O	2	8	2	8	2	8	2	8	2	8	THY
H_2O	3	9	3	9	3	9	3	9	3	9	THY
H_2O	4	10	4	10	4	10	4	10	4	10	THY
H_2O	5	11	5	11	5	11	5	11	5	11	THY
H_2O	6	12	6	12	6	12	6	12	6	12	THY
H_2O	H_2O	H_2O	H_2O	H_2O	H_2O	H_2O	H_2O	H_2O	H_2O	H_2O	H_2O

Figure 2.3: Plate organization of combinations during competition in broth. The figure illustrates how the samples of the twelve mixed cultures, depicted in orange, were organized on the plate to produce duplicates for sampling at 3 and 5 hours, and one sample from each mixed culture to be left for growth measurement. Depicted in blue, the outer wells of the plate were filled with distilled water (H_2O) to prevent evaporation of samples or, depicted in yellow, with THY to work as a blank control when measuring growth. The mixed cultures 1-12 is outlined in table 2.2.

Sampling of the mixed cultures was set at 0, 3, and 5 hours, and duplicates were made at each sampling point. The initial sampling at 0 hours was set as a control to check that each mixed culture consisted of approximately 50 % of each strain when starting the competition in broth. The sampling at 3 hours was set to measure concentration of each strain in the samples during mid-exponential phase, while the sampling at 5 hours was set to measure concentrations at peak exponential phase.

Immediately after sampling, all samples were prepared for DNA extraction, as described in section 2.3. On the day of extraction, samples were thawed on ice and further prepared for extraction through mechanical lysis, as described in section 2.3.1. Further, DNA was extracted, as described in section 2.3.2. Amplicon PCR of the housekeeping gene *gdh* was performed for all samples using the same PCR conditions as described in section 2.4.1. followed by purification of PCR products as described in section 2.4.4. Finally, samples were prepared and sent for Sanger sequencing as described in section 2.5.3.

After all samplings was conducted, one sample of each of the twelve different mixed cultures was left on the plate to measure their growth for a total of 20 hours, as illustrated in figure 2.3. When finished, the plate was discarded, and the data were exported to an Excel-file for further analysis.

2.8 Data analysis

2.8.1 Strain selection and characterization

Analyzation of the 16S sequencing results was done utilizing The Basic Local Alignment Search Tool (BLAST) for detection of similarity between the sequenced 16S rRNA amplicons and sequences in the database. Also, a cladogram depicting the phylogeny of the strains based on their 16S rRNA gene was generated through multiple sequence alignment (MSA) of the sequences using the program Clustal Omega (Sievers et al., 2011).

MSAs of the sequenced housekeeping genes were constructed using the program Clustal Omega (Sievers et al., 2011). The program marks homologous nucleotides in aligned sequences with "*" and single nucleotide polymorphisms (SNPs) with ".", ":", or " " depending on what type of mutation has occurred at the specific polymorphic site. MSAs of the sequenced housekeeping genes from all strains were transferred to Excel where MLST was conducted by all polymorphic sites being identified, numbered, and characterized, considering what type of SNP was observed.

Data from growth measurements using the plate reader was transferred to Excel where average growth was calculated for the six replicates of each strain. Average growth curves for all strains were made plotting the data into a line chart.

2.8.2 Statistical analysis of inhibitory effect during competition on plate

Diameter measurements of the inhibition zones were analyzed in Excel by calculating average size of inhibition zones produced by each strain and plotting the data into bar charts. The analysis involved comparison of zones produced by strains cultured on THY agar plates to those produced by strains cultured on TSA+SB plates, and the comparison of inhibition zones produced during the first and second round on competition on plate.

2.8.3 Calculating relative abundance of strains during competition in broth

When analyzing the Sanger sequencing results of the samples from competition in broth, the MLST results from the housekeeping gene *gdh* was conducted and a scoring system was created to decide the relative abundance of each strain in each of the mixed cultures. The nucleotide sequences from Sanger sequencing were submitted in the FASTA format, while the signal of each nucleotide in these sequences were illustrated graphically in PDFs. Sequences of the mixed samples were aligned with sequences generated from pure cultures of the three pneumococcal strains using Clustal Omega, and each polymorphic site was scored on a scale from 1-5 considering the nucleotide signals emitted at the specific site. As an example, figure 2.4 panel A illustrates a segment of a sequence alignment of the reverse nucleotide sequence of the housekeeping gene *gdh* in D39 and Hermans-33, including a mutation in Hermans-33 where a thymine (T) is replaced by a cytosine (C). All nucleotides at polymorphic sites within D39 was scored 1, while nucleotides at polymorphic sites in Hermans-33 was scored 5, as depicted in panel B. Further, panel C illustrates how the same segment of the nucleotide sequence is illustrated graphically for different samples after Sanger sequencing, with the polymorphic site scored differently in each sample based on the signals emitted.

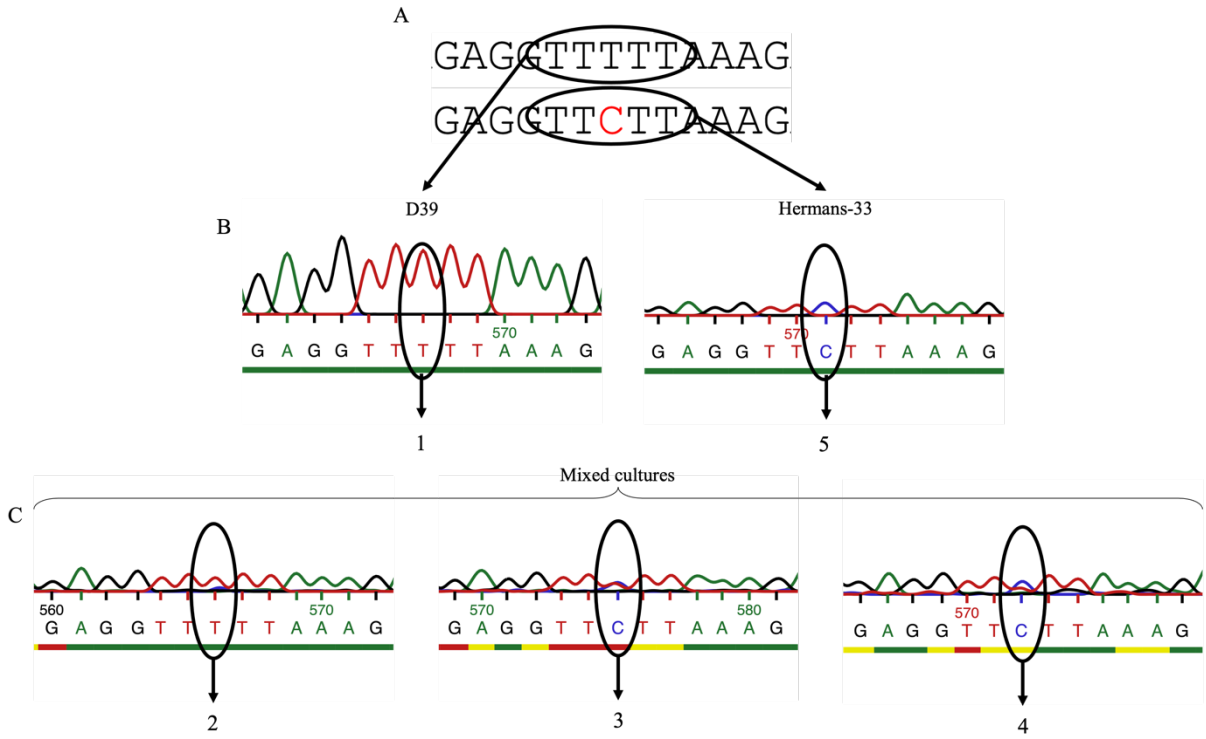

Figure 2.4: Scoring system to determine relative abundance of strains in mixed cultures. The figure illustrates (A) MSA of D39 and Hermans-33 with a polymorphic site scored in (B) pure cultures and (C) mixed cultures regarding the emitted nucleotide signal in samples. The signals emitted for each nucleotide during Sanger sequencing is shown as peaks colored based on the type of nucleotide.

Polymorphic sites that only signaled one nucleotide known to present the genome of one strain, was given the score 1, while polymorphic sites that only signaled a nucleotide known to be present in the genome of the other strain, was given the score 5. Also, polymorphic sites that signaled both nucleotides in the same position, indicated that the genomes of both strains were present in the sample. Most often, the signal for one nucleotide was higher than the other which means that the genomes of both strains are present in the sample, but in different quantity. As illustrated in the first example in figure 2.4 panel C, both T and C are signaled, but the signal for T is definitely bigger. Consequently, this mutation was given the score 2 as the abundance of the D39 was higher than that of Hermans-33. If the signal emitted for both nucleotides overlapped, the polymorphic site was given a score of 3, as illustrated in the next example. In the last example in figure 2.4 panel C, both T and C are signaled, but here the signal for C is bigger. As a results, this mutation was given the score 4 as the abundance of Hermans-33 is higher than D39.

After scoring all polymorphic sites among strains in mixed cultures, each sequence was given a number of scores considering the number of polymorphic sites between the two strains in the mixed culture. The mean of these scores was calculated for each sequence and translated to an approximate abundance scale from 0 to 1. Using a gene sequence from a mixed culture of D39 and PMEN-14 both cultured on TSA+SB, as an example, the sequence was given the score 2 at 0 hours, 3 at 3 hours at 4 at 5 hours. Given that nucleotides at polymorphic sites in D39 was represented by the score 1, this indicates that the sequence with an average score of 2 was more similar to D39 at 0 hours, than to PMEN-14. Consequently, the approximate abundance of D39 at 0 hours was 0.75, while it was 0.25 for PMEN-14. Further, at 3 hours, the sequence was given an average score of 3, which indicates that the sequence was represented equally by both strains regarding polymorphic sites, which yielded both strains an approximate abundance of 0.5. Finally, the sequence from the mixed culture sampled at 5 hours was given an average score of 4, which indicates that this sequence was more similar to PMEN-14, which had nucleotides at polymorphic sites represented by the score 5. The final approximate abundance of D39 in this mixed culture was 0.25, whereas it was 0.75 for PMEN-14.

3 RESULTS

3.1 Strain selection and characterization

3.1.1 16S sequencing

Sanger sequencing of the 16S rRNA gene in each strain confirmed that all strains were in fact *S. pneumoniae*. The phylogeny of the strains regarding their 16S rRNA gene is depicted in figure 3.1. The qualification control of the extracted DNA using gel electrophoresis confirmed the size of the amplicon to be around 1200 bp, as demonstrated in figure B.1 in appendix B.

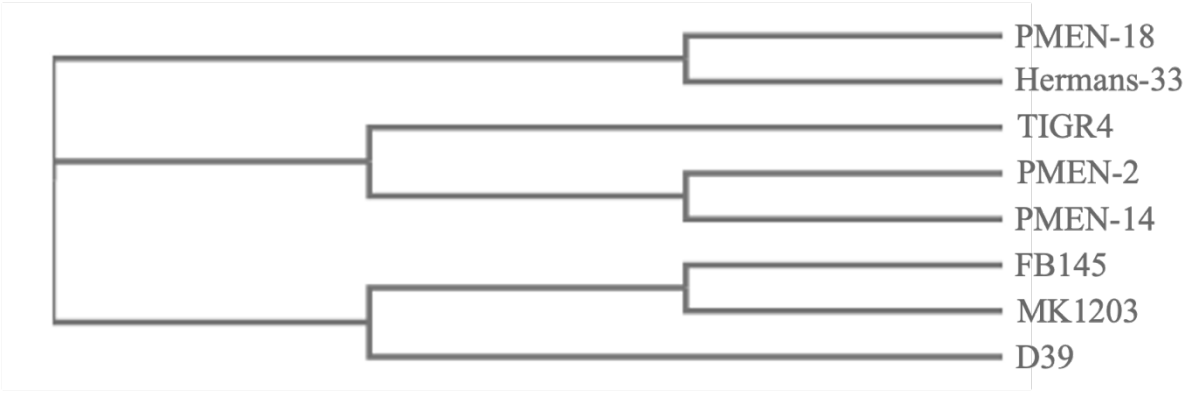

Figure 3.1: Cladogram of *S. pneumoniae* strains. The image displays a cladogram of the strains, generated by Clustal Omega using the sequences of their 16S rRNA gene obtained through Sanger sequencing.

3.1.2 Multiple sequence typing

MLST of the eight strains of *S. pneumoniae* revealed several single nucleotide polymorphisms (SNPs) within the sequenced housekeeping genes. Overall, the gene *gdh* yielded the most genetic variation among the eight strains, with the most diverse strains being D39, Hermans-33, and PMEN-14. Among these three strains, a total of 39 polymorphic sites were identified, numbered, and characterized considering the SNP observed at each site, as listed in table C.1 in appendix C.

3.1.3 Growth curves

The first round of growth measurements revealed notable differences in growth rate among the eight different strains, as depicted in figure 3.2. Most of the strains reached an exponential growth rate after around 2 hours and had a maximal OD_{600} between 0.7 to 0.9 after 5 hours. After, their growth slowly decreased and had almost halved for most of them after 20 hours. Compared to these strains, Hermans-33 showed a significant slower growth. This strain did not seem to grow like the other strains at all reaching an OD_{600} of almost 0.6 after 12 hours and keeping steady until reaching a small peak of OD_{600} just above 0.6 after 18 hours. Unfortunately, PMEN-14 did not seem to grow well, reaching a maximal OD_{600} of only a little less than 0.5. Its growth then decreased rapidly reaching an OD_{600} of around 0.1 after 16 hours.

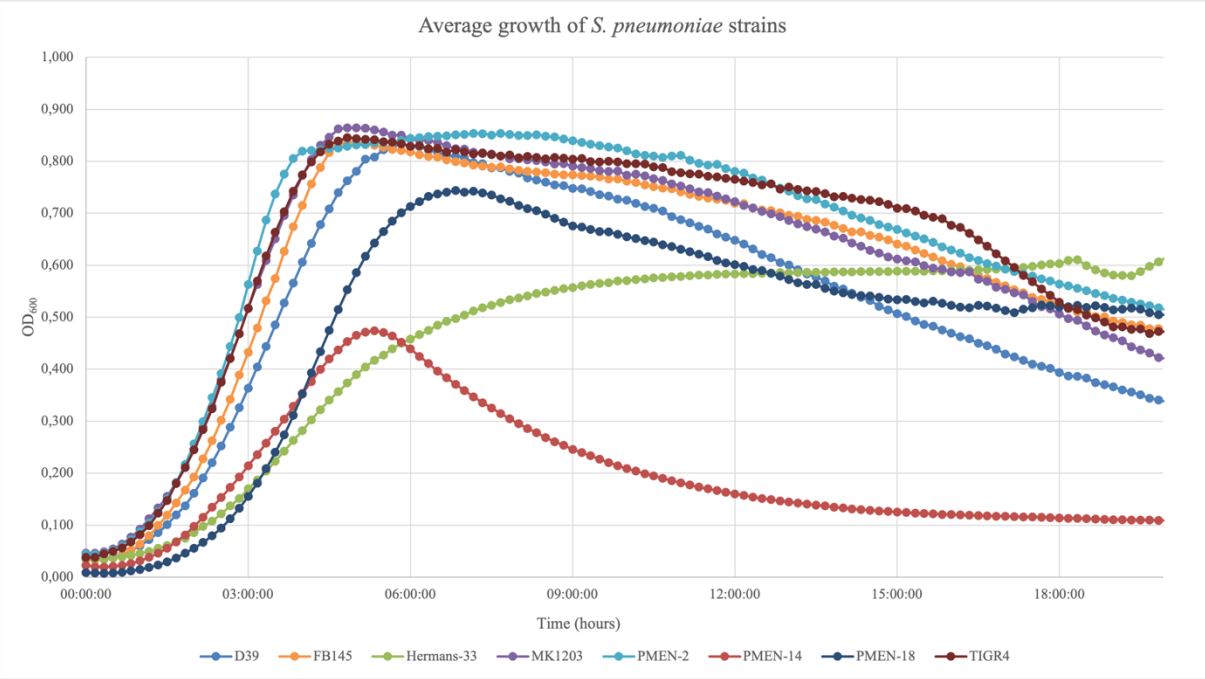

Figure 3.2: First round of growth curves. The graphs display the average growth of *S. pneumoniae* strains D39, depicted in blue, FB145, depicted in orange, Hermans-33, depicted in green, MK1203, depicted in purple, PMEN-2, depicted in turquoise, PMEN-14, depicted in red, PMEN-18, depicted in dark blue, and TIGR4, depicted in burgundy. Each graph represents an average of six duplicates of each strain. The x-axis represents time in hours, while the y-axis represents OD_{600}.

The second round of growth measurements only included the three strains that were picked out for further competitive investigation, including D39, Hermans-33, and PMEN-14, as depicted in figure 3.3. This time PMEN-14 grew to a higher OD_{600} with an almost identical exponential growth as D39. Both strains started growing exponentially after 2 hours and reached a maximal OD_{600} of 0.8 after between 4 and 5 hours. D39 decreased slowly with an OD_{600} of 0.48 after 20 hours, whereas PMEN-14 exhibited a more rapid decrease in growth reaching an OD_{600} of 0.27 after 20 hours. Similar to the first round, Hermans-33 showed a very different growth pattern than the other strains, reaching exponential growth phase after 5 hours. This strain reached its maximal OD_{600} of 0.5 after 16 hours and kept a steady growth until 20 hours had passed.

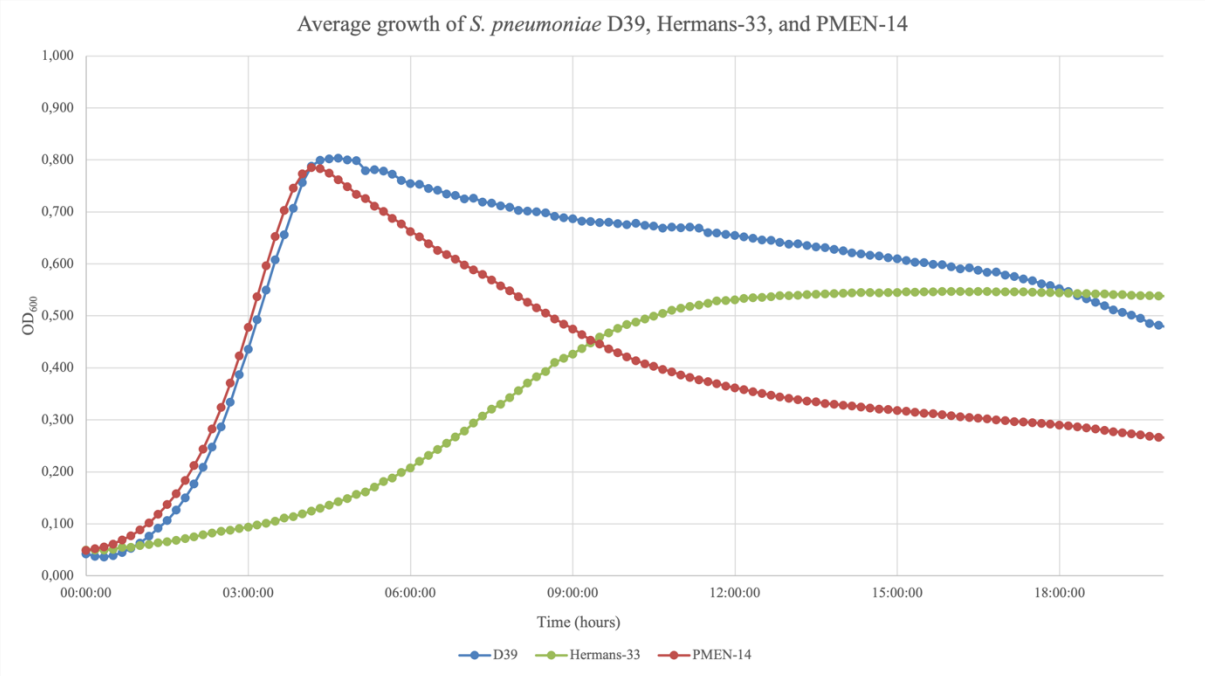

Figure 3.3: Second round of growth curves. The graphs display the average growth of *S. pneumoniae* strains D39, depicted in blue, Hermans-33, depicted in green, and PMEN-14, depicted in red. Each graph represent an average of six replicates of each strain. The x-axis represents time in hours, while the y-axis represents OD_{600}.

3.1.4 Microscopy

The microscopy of the individual strains displayed noticeable differences in morphology. As depicted inn figure 3.4 panel A, D39 is shown mostly as diplococci but also as single cells. On the other hand, Hermans-33, in panel B, is mostly shown as chains of four or more cells. Lastly, in panel C, PMEN-14 is shown similar to D39, but in a lower concentration of cells.

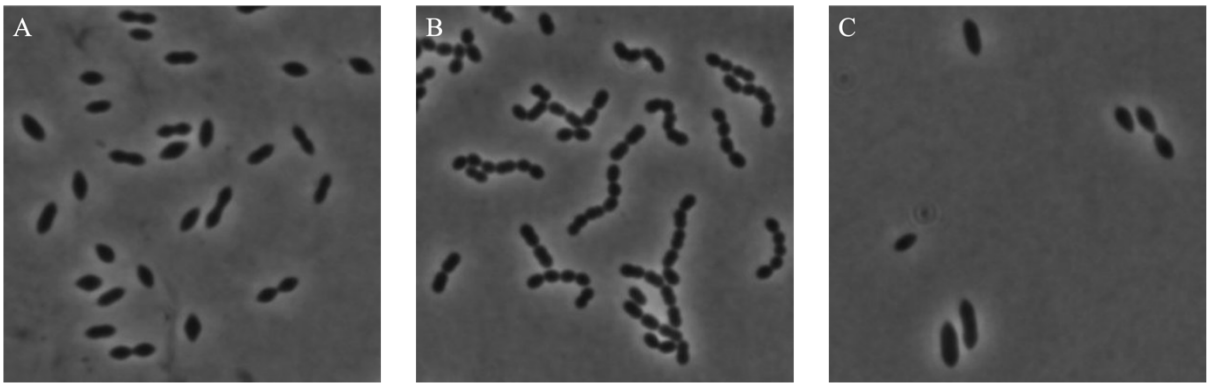

Figure 3.4: Microscopy pictures of *S. pneumoniae* strains. The pictures taken utilizing the Zeiss LSM 700 microscopy reveal morphology of strains (A) D39, (B) Hermans-33, and (C) PMEN-14 when diluted in PBS after O/N incubation on TSA at 37°C with 5 % CO_2.

3.2 Competition experiments

3.2.1 Competition on plate

The results from the first round of competition on plate revealed notable differences in size of inhibition zones generated by the eight strains initially cultured on THY and TSA+SB plates, as summarized in table E.1 and E.2 appendix E. Hermans-33 generated larger inhibition zones compared to all the other strains, yielding zones with an average diameter of 6.2 mm. The overlay assays with D39, Hermans-33, and PMEN-14 are depicted in figure 3.5, whereas the overlay assays with the remaining strains are depicted in figure E.1 in appendix E. PMEN-14 did not grow in the overlay, thereby inhibition zones of this strain were not applicable (N/A).

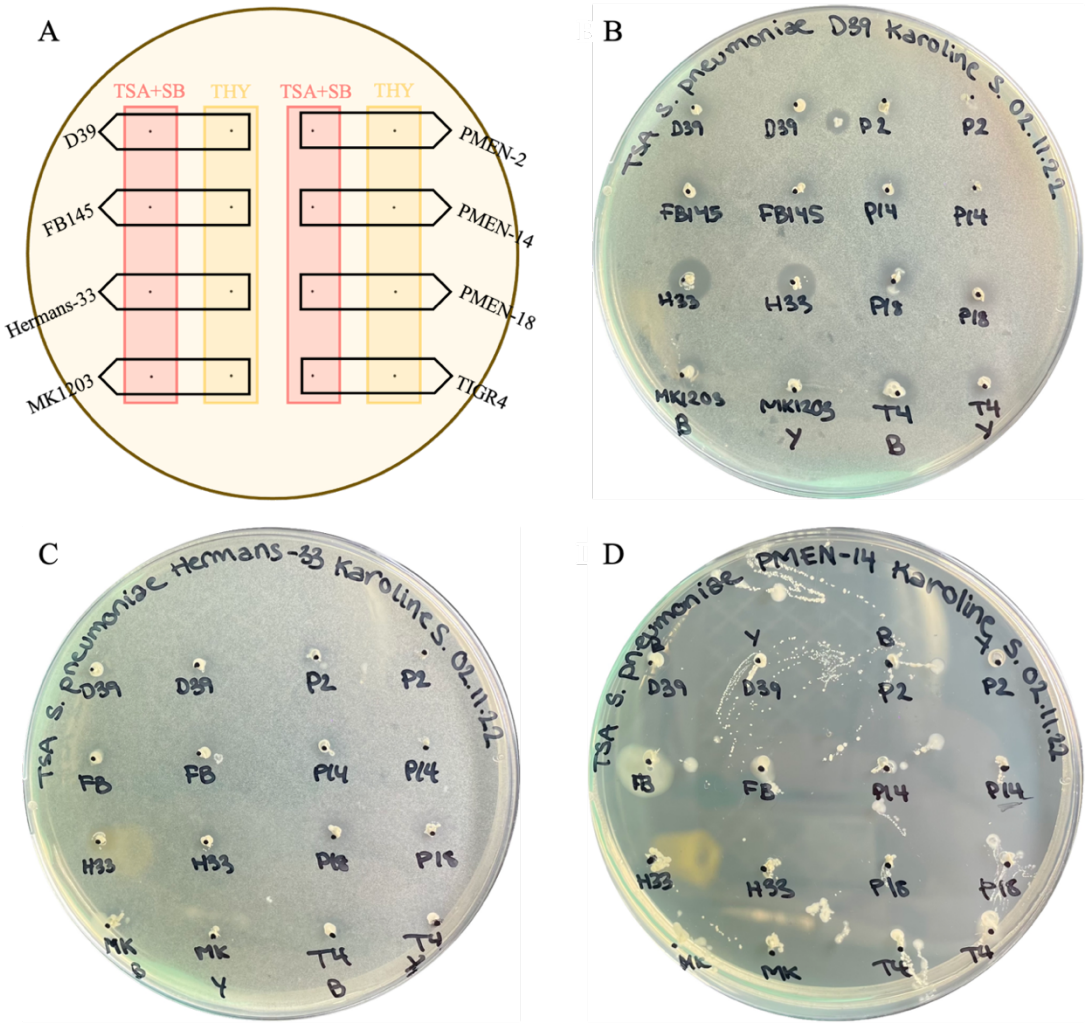

Figure 3.5: Overlay assays after first round of competition on plate. The figure displays (A) illustration of how each plate was stabbed with each producer strain two times, one initially cultured on THY agar and the other on TSA+SB, followed by results from the first round of competition on plate with (B) D39, (C) Hermans-33, and (D) PMEN-14 as the overlay strain. PMEN-14 did not grow in the overlay, thereby the clear overlay.

Additionally, the first round of competition on plate unveiled a variation in the inhibition zones generated by the stabbed strains grown on THY plates compared to those produced by strains grown on TSA+SB plates. Displayed in figure 3.6, the average diameter of the inhibition zones produced by strains cultured on TSA+SB plates was larger for 7 out of 8 strains compared to those produced by strains cultured on THY plates. Strains incubated O/N at TSA+SB plates all exhibited α-hemolysis, as displayed in figure C.1 in appendix C.

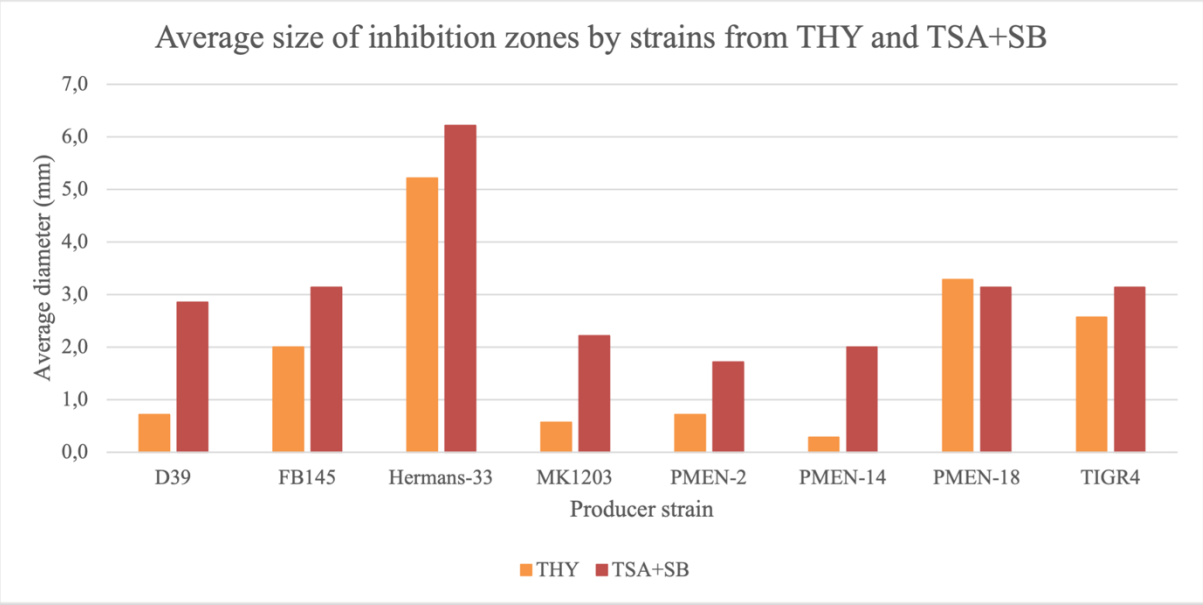

Figure 3.6: Comparison of inhibition zones produced by strains cultured on THY and TSA+SB. The bar chart displays the average diameter size of the inhibition zones produced by each strain initially cultured on THY plates, depicted in orange, compared to those produced by each strain initially cultured on TSA+SB plates, depicted in red.

The results from the second round of the competition on plate indicated the same variation in inhibitory effect among the strains, as summarized in table E.3 in appendix E. Again, Hermans-33 produced the largest inhibition zones with an average diameter size of 5.1 mm. The overlay assays with D39, Hermans-33, and PMEN-14 are depicted in figure 3.7, whereas the overlay assays with the remaining strains are depicted in figure E.2 in appendix E.

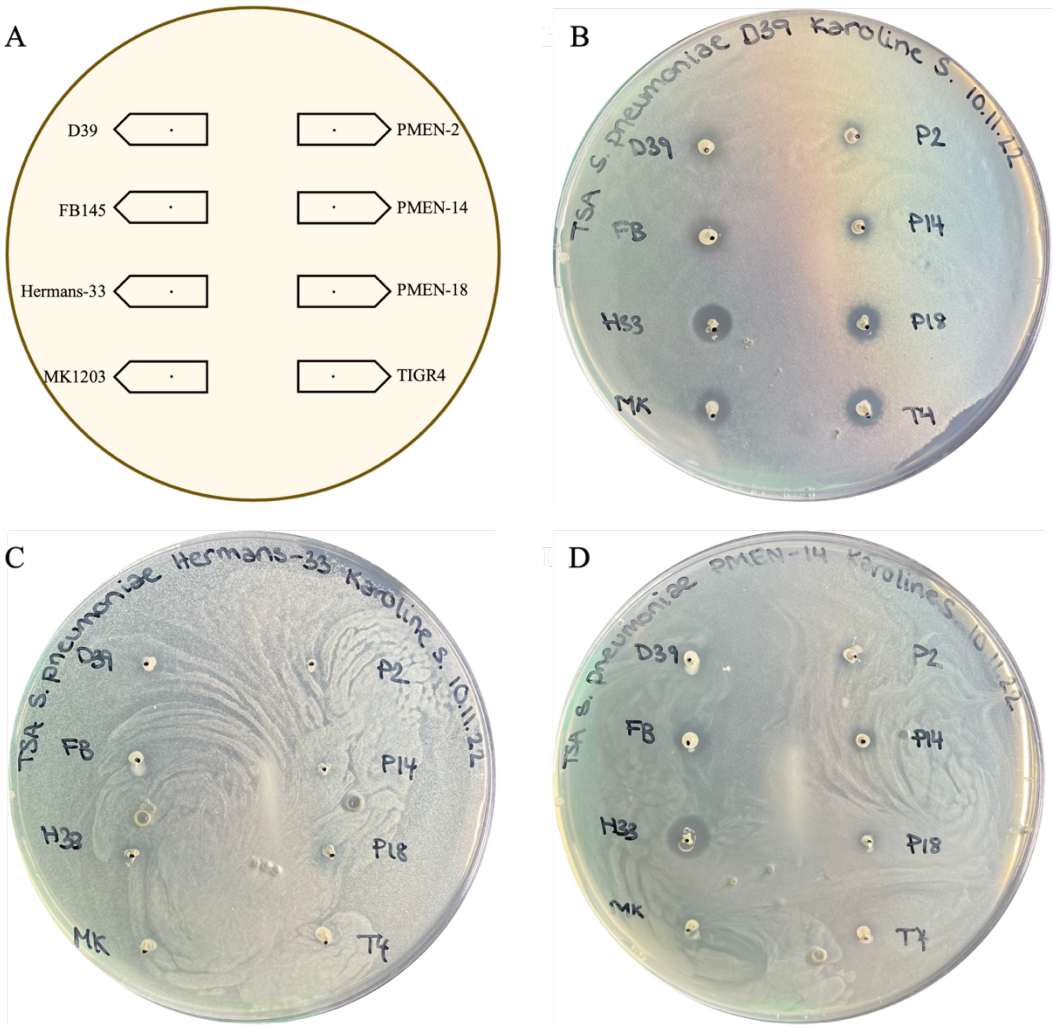

Figure 3.7: Overlay assays after second round of competition on plate. The figure displays (A) illustration of how each plate was stabbed with each producer strain initially cultured on TSA+SB, followed by results from the second round of competition on plate with (B) D39, (C) Hermans-3, and (D) PMEN-14 as the overlay strain.

Comparison of the inhibition zones generated by producer strains initially cultivated on TSA+SB plates during the first and second round of competition on plate revealed the same pattern regarding the size of the zones produced be each strain in both experiments, as depicted in figure 3.8.

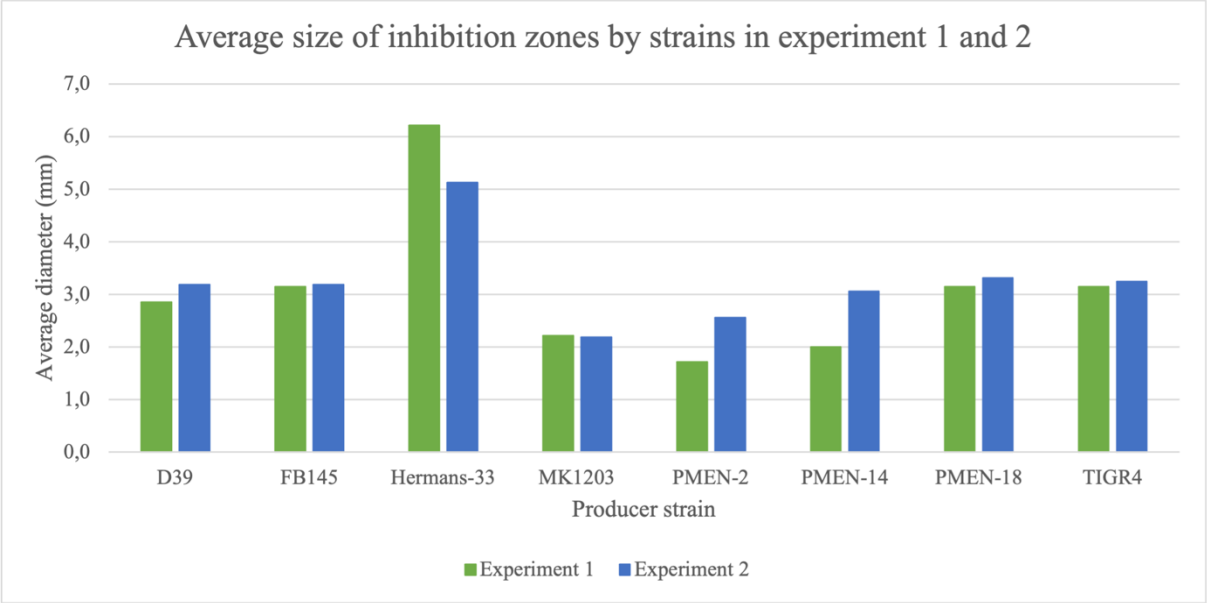

Figure 3.8: Comparison of inhibition zones in first and second round of competition on plate. The bar chart displays the average diameter size of the inhibition zones produced by each strain in experiment 1, depicted in green, compared to those produced in experiment 2, depicted in blue.

3.2.2 Competition in broth

The competition in broth revealed a consistent pattern regarding which strain would dominate the broth over time. Independent of what type of agar strains were cultured on before grown to exponential growth phase in THY, a mean relative abundance of each strain in mixed cultures, displayed in figure 3.9, was calculated for all three sampling points during competition in broth. Approximate relative abundance of each strain in all mixed cultures are summarized in table F.1 in appendix F and illustrated in figure F.1, F.2, and F.3.

The initial sampling point at 0 hours produced noninterpretable results in eight out of the 24 samples analyzed. In the remaining 16 samples, only six cultures indicated an equal quantity of both strains at the beginning of the experiment. The mixed cultures of D39 and Hermans-33 consistently revealed the same competitive outcome, with D39 surpassing Hermans-33 within 3 hours in six out of eight samples, or within 5 hours in the remaining two samples. Further, the interpretation of the mixed cultures comprised of D39 and PMEN-14 indicated a less superior competitive outcome. Here, the relative abundance of both strains was 0.5 in three out of eight samples at 3 hours, while PMEN-14 dominated the broth at a relative abundance of 0.75 in the remaining five. At 5 hours, PMEN-14 dominated D39 with a relative abundance of 0.75 in a six out of eight samples. One sample at 5 hours included both strains in equal amounts, while the last one was actually dominated by D39 at a relative abundance of 0.75. Lastly, the mixed cultures of Hermans-33 and PMEN-14 demonstrated the most superior competitive outcome observed during the competition in broth. At 3 hours, Hermans-33 was completely outgrown by PMEN-14 in as many as six out of eight samples, while the remaining two samples at this sampling point was dominated by PMEN-14 at a relative abundance of 0.75. Finally, at 5 hours, all samples initially comprised of PMEN-14 and Hermans-33 indicated that PMEN-14 had fully outcompeted Hermans-33.

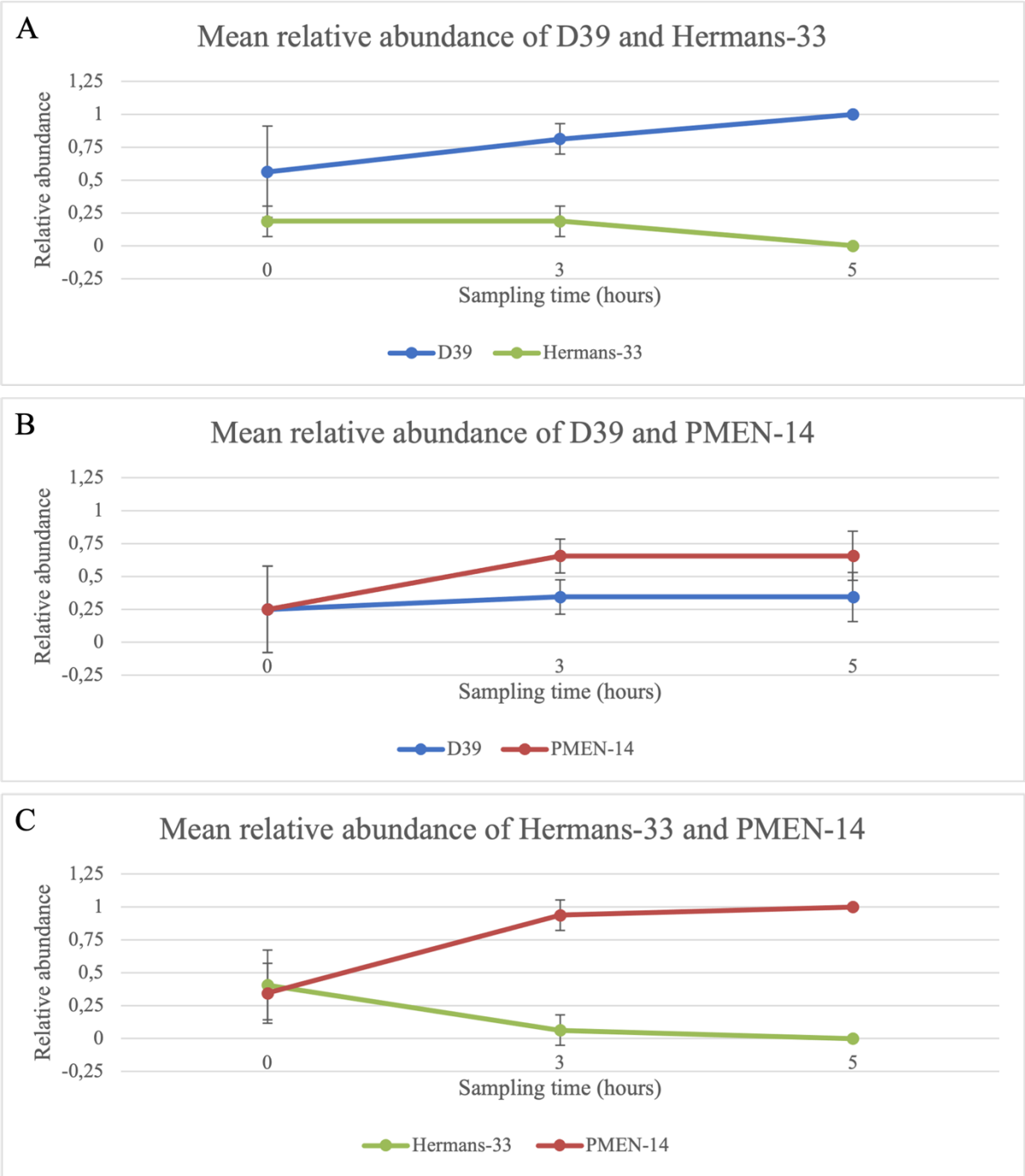

Figure 3.9: Mean relative abundance of strains during competition in broth. The graphs illustrate mean relative abundance in mixed cultures of (A) of D39, depicted in blue, and Hermans-33, depicted in green, (B) D39, depicted in blue, and PMEN-14, depicted in red, (C) Hermans-33, depicted in green, and PMEN-14, depicted in red, in mixed cultures at 0, 3, and 5 hours during the competition in broth.

Growth curves of the mixed cultures indicated a trend where the samples consisting of strains cultured on the same type of agar media tended to reach a higher maximum OD_{600} than samples consisting of strains cultured on different type of agar, as displayed in figure 3.10.

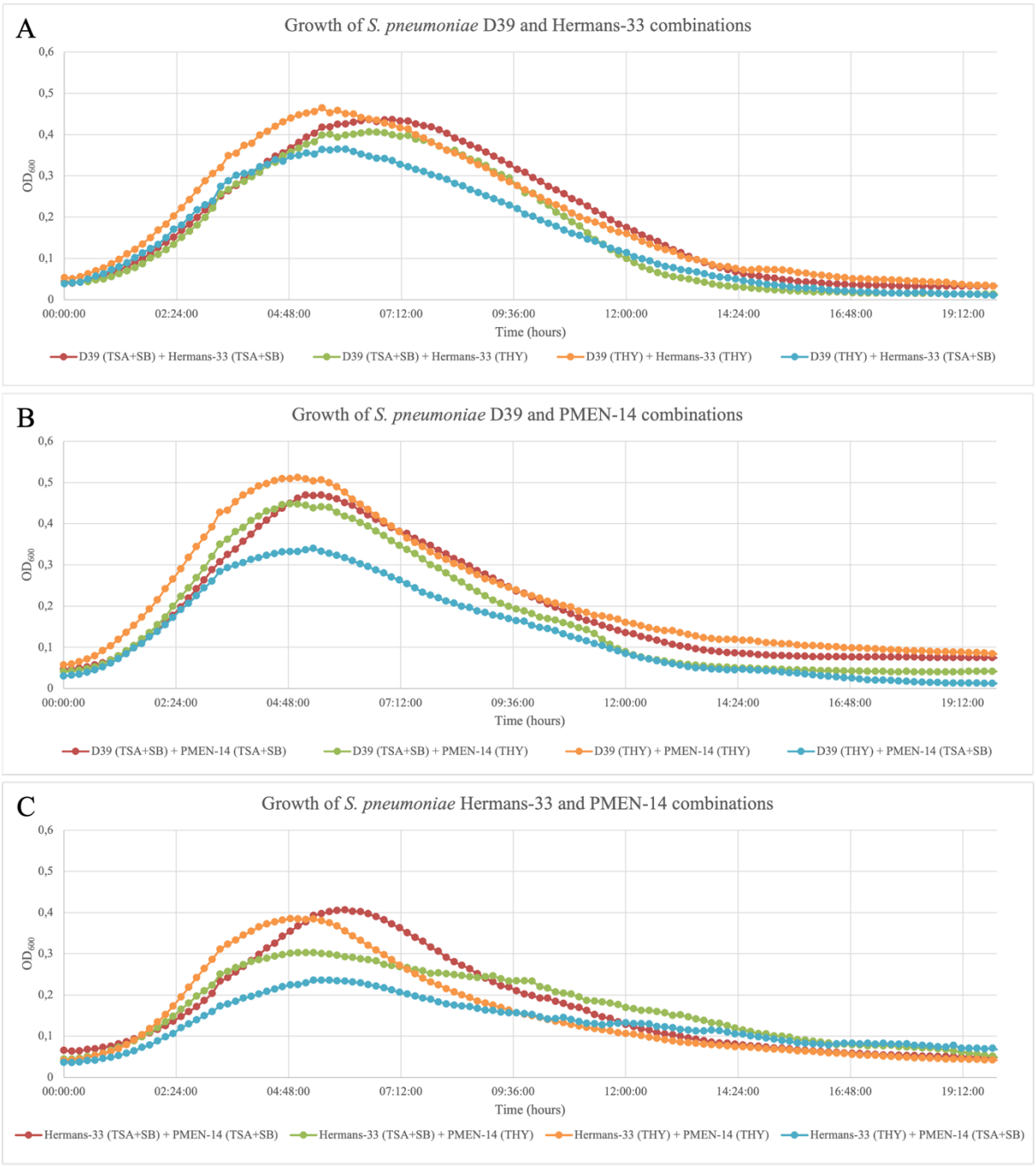

Figure 3.10: Growth curves of mixed cultures. The graphs display the growth curves of mixed cultures comprised of (A) D39 and Hermans-33, (B) D39 and PMEN-14, and (C) Hermans-33 and PMEN-14. In all panels, red graphs illustrate growth of mixed strains both initially cultured on TSA+SB, orange graphs illustrate growth of mixed strains both initially cultured on THY, and green and blue graphs illustrate graphs of mixed strains initially cultured on different type of agar media. The x-axis represents time in hours, while the y-axis represents OD_{600}.

4 DISCUSSION

4.1 *S. pneumoniae* strains exhibit varying competitiveness in diverse media

4.1.1 Strain diversity could potentially be explained by r/K selection theory

The primary discovery of this research was the contrasting competitive outcomes observed for the strains in the two conducted competition experiments. The three strains of *S. pneumoniae*, D39, Hermans-33, and PMEN-14, exhibited different competitive characteristics during competition on plate than during competition in broth. Competition on plate revealed varying outcomes concerning the inhibitory potential of each producer strain. The experiment was conducted twice, and in both instances, Hermans-33 consistently demonstrated significantly higher inhibition capacity compared to all other strains, as illustrated in figure 3.8. In contrast to these results, competition in broth demonstrated that Hermans-33 was surpassed by both D39 and PMEN-14 within a matter of hours, as illustrated in figure 3.9.

The r/K selection theory could potentially explain the outcomes witnessed in the separate competition experiments, implying that Hermans-33 is a K-strategist, and that D39 and PMEN-14 are r-strategists. As described in section 1.1.3, there are two distinct reproductive strategies among all living organisms, called r-selection and K-selection. The observed results indicate that Hermans-33 thrives in environments with a high bacterial density, as seen on agar plates, whereas the other two strains, D39 and PMEN-14, thrive in environments with a lower bacterial density, as presented in liquid broth. Within high-density environments, organisms possessing advantageous traits, such as inhibitory capabilities, could potentially outcompete those lacking such beneficial attributes, either in the form of equivalent capabilities or immunity-providing agents. Conversely, within low-density environments, organisms exhibiting rapid growth rates will eventually surpass those with relatively slower growth rates.

4.1.2 Previous research on intraspecific competition within *S. pneumoniae*

In 2010, a study by Freilich et al. delved into bacterial ecological communities, revealing a pattern of minimal competition in rapidly growing communities and heightened competition in slower growing communities. The study proposed the r/K selection theory to elucidate these findings, attributing rapid growth to r-strategists and competitive adaptation to K-strategists, particularly in resource-scarce conditions. The results by Freilich et al. indicated that gut bacteria aligned more with r-strategists, whereas pathogens and symbionts leaned towards K-strategists. A suggested plausible interpretation was that pathogens and symbionts adopt a strategy of avoiding excessive resource consumption in their host, thereby preserving their protective niche (Freilich et al., 2010).

In 2018, Miller et al. unveiled that *in vitro* social interactions could yield complex ecological outcomes that potentially influences strain diversity within the species of *S. pneumoniae*. The research involved investigation of the QS mediated bacteriocin expression among pneumococci and discovered that crosstalk, meaning cells produced signals detected by other strains, did occur among strains. Additionally, they observed eavesdropping, a phenomenon where cells responded to signals produced by others, was proven as beneficial when cells were surrounded by reliable strains, as opposed to competing strains that induced bacteriocin production at densities too low to provide satisfactory effects, thus avoiding the cost of overproduction. Although the research of this thesis did not identify bacteriocins as potential mechanisms explaining strain diversity within the infant gut, they are believed to play an important role in mediating intraspecific competition among pneumococcal strains (Miller et al., 2018).

During another study, Kuhn et al. explored the impact of spatial scales on competition dynamics through the creation of two distinct heterogeneous environments featuring biotic and abiotic dispersal networks. By examining two closely related strains of *Pseudomonas putida*, they demonstrated how local competition triggered competitive exclusion, whereas regional competition facilitated coexistence. These findings shed light on how the spatial organization of competing strains, given their overlapping niches, influence the competitive outcome (Kuhn et al., 2022). Throughout the research conducted in this thesis, strain competition was examined in two distinct environments, including agar plates and liquid broth, which provide the bacteria with different spatial conditions. While the specific environments compared in this research differ from those compared in the study by Kuhn et al., the possibility of spatial organization of strains as a contributory factor for strain diversity cannot be dismissed.

As mentioned in the aim of this thesis, a recent study by Ormaasen et al. discovered a correlation of strain diversity and the presence of genes encoding specific bacteriocins in the infant human gut (Ormaasen et al., 2023). A suggested explanation for these findings was the intransitive ecological model of coexistence resembling the children's game of rock-paper-scissors (RPS), where rock crushes scissors, scissors cut paper, and paper covers rock (Kerr et al., 2002). In microbiology, a hypothetical scenario of RPS could involve a sensitive strain outcompeting an immune strain by avoiding the cost of immunity proteins, an immune strain surpassing a bacteriocin-producer by avoiding the cost of bacteriocin production while remaining resistant to bacteriocins, and a bacteriocin-producer prevailing over a sensitive strain through production of bacteriocins. Such a scenario demonstrates no winning strategy among the various strains, potentially facilitating coexistence and strain diversity (Abrudan et al., 2012).

The competitive outcomes observed in this study of this thesis do not align with an RPS scenario. However, they are not contradictory to the findings by Ormaasen et al., which were conducted by analyzing metagenomes of the gut. Metagenomes represent the total genetic material within an environment (Thomas et al., 2012), and considering the diverse environments within the human gut, strains exhibiting different strategies could be maintained at overall similar abundances within the gut due to their possession of advantageous properties suited to different conditions. Thus, reproductive strategies adopted by bacterial strains are ecological mechanisms that could potentially explain the high strain diversity of *S. pneumoniae* within the human infant gut.

4.2 Type of agar medium influenced the competitive outcome

Throughout the research of this thesis, pneumococcal strains were cultured on both blood-enriched and yeast-enriched agar plates to test if the competitive outcome was influenced by the media. Results revealed that the type of agar media does in fact influence the competitive outcome of intraspecific competition among strains of *S. pneumoniae*.

4.2.1 Blood stimulated greater inhibition than yeast

The first round of competition on plate revealed a trend where producer strains cultured on TSA+SB, which is blood-enriched agar, consistently generated larger inhibition zones in the overlay strains compared to those cultured on THY, which is yeast-enriched agar, as illustrated in figure 3.6. This observation aligns with its role as a common human pathogen and the preference for blood-enriched media among streptococci in general (Patterson, 1996)

4.2.2 Strains cultured on same type of agar media expressed higher growth in broth

Unlike the competitive patterns observed on agar plates, the competitive results in liquid broth did not demonstrate a consistent trend of strains exhibiting a stronger competitive outcome when cultured on TSA+SB compared to THY. However, the growth curves of the mixed strain samples revealed another interesting pattern where the mixed cultures composed of strains initially cultivated on the same type of agar medium tended to reach higher OD_{600} than those grown on different types of agar media. This pattern was observed in all three pairs of mixed cultures, as displayed in figure 3.10, and could indicate that the mixed cultures of strains both initially cultured on THY required less time to adjust to the liquid THY, whereas those of strains both initially cultured on TSA+SB was provided more nutrients and thereby an advantage as observed during the first round of competition on plate.

4.3 Growth curves unveils behavioral variations

4.3.1 Comparison of growth curves of pure cultures

Comparisons of growth curves of pure cultures unveils variations in rate and pattern of growth in liquid broth between specifically one strain and the rest. Compared to all other strains, Hermans-33 did not reach exponential growth phase before several hours later compared to the others and kept a stationary growth throughout the whole growth experiment of a total of 20 hours, as displayed in figure 3.2 and 3.3. This observation demonstrated how Hermans-33, compared to all the other strains included in this research, exhibited a significantly lower growth rate when grown in liquid media.

4.3.2 Pure cultures exhibited higher growth rate than mixed cultures

Growth measurements reveals significantly higher OD_{600} when strains are grown as pure cultures compared to when they are mixed. In a competitive situation, strains will prioritize using their energy and resources to compete against the other strain rather than reproducing, and the observed variations in growth rate of pure cultures opposed to mixed cultures is thereby a clear indicator of competition.

4.3.3 Previous research on growth curves of mixed cultures

Growth curve experiments of mixed cultures can be more demanding and expensive than growth curve experiments of pure cultures due to the requirement of genetic or phenotypic markers. To solve this, Ram et al., 2019 developed a model-based approach for prediction of microbial growth in a mixed culture and relative fitness using data from growth curves. In the development this approach, *Escherichia coli* was used as a model organism and competition coefficients were considered. The approach included the assumption that mixed strains will grow in a density-dependent manner, meaning growth depend on the availability of resources. Conversely, it was not appropriate for strains exhibiting frequency-dependent growth, such as pneumococci performing QS mediated communication (Ram et al., 2019). Considering pneumococcal strains are known to communicate in a QS manner, as demonstrated by Miller et al., this approach did not fit the growth of the strains used in the study of this thesis.

4.4 Methodological considerations of this research

Throughout the research of this thesis, and upon reflection, various considerations have been contemplated regarding the optimization of the methodology and need to be addressed.

4.4.1 *S. pneumoniae* is not a typical gut bacterium

Within the human gut there are several bacterial species representing the core microbiota, like for instances *Bifidobacteria* and *Bacteroides* (Milani et al., 2017). *S. pneumoniae* is not the most abundant species within the human gut microbiota, but it is found to be present at smaller abundances (Ormaasen et al., 2023). As mentioned in section 1.2.1, pneumococci are most abundant in the human nasopharynx and thereby adapted for conditions as seen in this environment. However, *S. pneumoniae* was chosen considering recent discoveries regarding its diversity in the infant human gut and the availability of established methods and material, as described in section 1.4.

4.4.2 Conflicting considerations regarding selection of competing strains

During strain selection and characterization of the *S. pneumoniae* strains, it was demonstrated that strains of this species does not necessarily behave or look the same. The microscopy performed revealed great variations in organization among the three strains. While D39 and PMEN-14 occurred mostly as diplococci, Hermans-33 mostly occurred as chains of four cells or more. Additionally, when measuring growth of the strains, Hermans-33 exhibited a significantly different growth pattern than the others, as displayed in figure 3.2 and 3.3. Considering this variation in growth rate, Hermans-33 should not have been included to have fair competition. On the other hand, it was interesting to test its inhibition capability in liquid media after witnessing its inhibitory effect towards other strains on solid agar. Genetic analysis using MLST of the sequenced housekeeping genes revealed a number of polymorphic sites among the eight different strains. The gene *gdh*, contained the highest number of polymorphic sites, with D39, Hermans-33, and PMEN-14 being the most genetically diverse strains. In the end, after considering variations in growth patterns and inhibition capability on plate, the ability to identify and differentiate strains in a mixed culture emerged as a pivotal factor regarding interpretation of results.

4.4.3 The scoring system of Sanger sequences was not an accurate approach

Data analysis of the results from competition in broth turned out to be a time-consuming task in need of a self-constructed scoring system to interpret the Sanger sequences of samples with different genomes. This approach of determining relative abundance of two strains in a mixed population over time is not an accurate approach, but rather an approximate approach developed to roughly interpret Sanger sequencing results. Additionally, when conducting the competition in broth, samples of mixed cultures were taken at an OD_{600} of only 0.05. Considering cultures were grown to an OD_{600} of 0.3-0.5 ahead of previous extractions, the number of cells at OD_{600} of 0.05 was expected to generate Sanger sequences of low quality. The gel pictures in figure B.2-B.7 reveals less visible bands of *gdh* in mixed cultures sampled at 0 hours, compared to those sampled at 5 hours. This was potentially the reason that eight out of 24 mixed cultures had an average abundance of 0 for each strain at 0 hours. To prevent this, several PCR cycles could have increased the DNA concentrations in these samples (Trosvik et al., 2007).

4.4.4 Limitations regarding quantification during experiments

During competition on plate, visible amounts of bacteria were stabbed into the agar using pipette tips. Thereby, the number of bacteria producing inhibition zones could have varied among strains. Additionally, when conducting the experiment in broth, pure cultures of strains were mixed at a 1:1 ratio, but the calculated relative abundance of each strain at 0 hours, as depicted in table F.1, indicated that only six out of 16 interpretable samples had equal quantities of both strains starting the experiment. These factors could potentially influence the competitive patterns observed during this research.

4.4.5 Laboratory environments do not equal *in vivo* conditions

Experiments conducted in the laboratory do not represent natural environments and bacteria might not necessarily behave the same way *in vivo* as they do during research performed in a sterile laboratory. Likewise, the agar plates and the liquid broth used as models during this research, are not the same as complex mucosal surfaces or the intestinal lumen. The study by Ormaasen et al. analyzed metagenomes of bacteria in their *in vivo* conditions, while the research conducted in this thesis investigated competitive mechanisms among bacteria under *in vitro* conditions. Given the complexity of the gut environment, especially due to the numerous amounts of species inhabiting it and the interactions among them, it is difficult to create realistic models simulating *in vivo* conditions. However, laboratory experiments works as preliminary studies to establish optimized models for *in vivo* studies.

5 CONCLUSION

This study identified significant variations in competitive patterns among different strains of *S. pneumoniae* during competition on agar plate and in liquid broth.

The primary discovery is the difference in competitive outcomes for pneumococcal strains during competition on plate compared to during competition in broth. Hermans-33 exhibited higher inhibitory capabilities compared to all other strains included during competition on plate, whereas it was outcompeted by both D39 and PMEN-14 during competition in broth. Conversely, D39 and PMEN-14 were among the strains exhibiting the least inhibition of other strains during competition on plate, while they both completely surpassed Hermans-33 during competition in broth. A suggested explanation for these findings is the reproductive strategies of r/K selection theory, implying that D39 and PMEN-14 are r-strategists, whereas Hermans-33 is a K-strategist. The characteristic properties of r-strategists include high growth rates and low competitive abilities, as observed in both D39 and PMEN-14 during intraspecific competition, whereas typical characteristics of K-strategists include low growth rates and highly competitive abilities, as observed in Hermans-33 during intraspecific competition. Given the heterogenous environments within the human infant gut, strains exhibiting different strategies due to their possession of distinct characteristics could be maintained at an overall similar abundance. Another discovery involved the variation in inhibitory effect of *S. pneumoniae* strains initially cultured on blood-enriched agar as opposed to those cultured on yeast-enriched agar, where blood consistently yielded greater inhibition than yeast. A suggested explanation for this finding is the role of *S. pneumoniae* as a common human pathogen and thereby its preference for blood-based media. Additionally, a pattern of pure cultures exhibiting higher growth than mixed cultured was observed, with the proposed explanation being bacteria down prioritizing growth during competitive settings.

In conclusion, the reproductive strategy adopted by bacterial strains is an ecological mechanism that could potentially explain the high diversity of *S. pneumoniae* strains within the infant human gut. However, future research is suggested to further explore these competitive outcomes, for instance involving the detection of substances yielding inhibition. Also, species more abundant in the human infant gut should be investigated.

References

Abrudan, Monica I., Brown, S., & Rozen, Daniel E. (2012). Killing as means of promoting biodiversity. *Biochemical Society Transactions*, *40*(6), 1512-1516. https://doi.org/10.1042/BST20120196

Aggarwal, S. D., Yesilkaya, H., Dawid, S., & Hiller, N. L. (2020). The pneumococcal social network. *PLOS Pathogens*, *16*(10), e1008931. https://doi.org/10.1371/journal.ppat.1008931

Alvarez-Sieiro, P., Montalbán-López, M., Mu, D., & Kuipers, O. P. (2016). Bacteriocins of lactic acid bacteria: extending the family. *Applied Microbiology and Biotechnology*, *100*(7), 2939-2951. https://doi.org/10.1007/s00253-016-7343-9

Andrews, J. H., & Harris, R. F. (1986). r- and K-Selection and Microbial Ecology. In K. C. Marshall (Ed.), *Advances in Microbial Ecology* (pp. 99-147). Springer US. https://doi.org/10.1007/978-1-4757-0611-6_3

Avershina, E., Lundgård, K., Sekelja, M., Dotterud, C., Storrø, O., Øien, T., Johnsen, R., & Rudi, K. (2016). Transition from infant- to adult-like gut microbiota. *Environ Microbiol*, *18*(7), 2226-2236. https://doi.org/10.1111/1462-2920.13248

Bentley, S. D., Aanensen, D. M., Mavroidi, A., Saunders, D., Rabbinowitsch, E., Collins, M., Donohoe, K., Harris, D., Murphy, L., Quail, M. A., Samuel, G., Skovsted, I. C., Kaltoft, M. S., Barrell, B., Reeves, P. R., Parkhill, J., & Spratt, B. G. (2006). Genetic analysis of the capsular biosynthetic locus from all 90 pneumococcal serotypes. *PLoS Genet*, *2*(3), e31. https://doi.org/10.1371/journal.pgen.0020031

Biagi, E., Aceti, A., Quercia, S., Beghetti, I., Rampelli, S., Turroni, S., Soverini, M., Zambrini, A. V., Faldella, G., Candela, M., Corvaglia, L., & Brigidi, P. (2018). Microbial Community Dynamics in Mother's Milk and Infant's Mouth and Gut in Moderately Preterm Infants [Original Research]. *Frontiers in Microbiology*, *9*. https://doi.org/10.3389/fmicb.2018.02512

Chao, Y., Marks, L. R., Pettigrew, M. M., & Hakansson, A. P. (2014). Streptococcus pneumoniae biofilm formation and dispersion during colonization and disease. *Front Cell Infect Microbiol*, *4*, 194. https://doi.org/10.3389/fcimb.2014.00194

Clarridge, J. E., 3rd. (2004). Impact of 16S rRNA gene sequence analysis for identification of bacteria on clinical microbiology and infectious diseases. *Clin Microbiol Rev*, *17*(4), 840-862, table of contents. https://doi.org/10.1128/cmr.17.4.840-862.2004

Dewey, F. E., Pan, S., Wheeler, M. T., Quake, S. R., & Ashley, E. A. (2012). DNA sequencing: clinical applications of new DNA sequencing technologies. *Circulation*, *125*(7), 931-944. https://doi.org/10.1161/circulationaha.110.972828

Differding, M. K., & Mueller, N. T. (2020). Human Milk Bacteria: Seeding the Infant Gut? *Cell Host Microbe*, *28*(2), 151-153. https://doi.org/10.1016/j.chom.2020.07.017

Dogra, S., Sakwinska, O., Soh, S. E., Ngom-Bru, C., Brück, W. M., Berger, B., Brüssow, H., Lee, Y. S., Yap, F., Chong, Y. S., Godfrey, K. M., & Holbrook, J. D. (2015). Dynamics of infant gut microbiota are influenced by delivery mode and gestational duration and are associated with subsequent adiposity. *mBio*, *6*(1). https://doi.org/10.1128/mBio.02419-14

Freilich, S., Kreimer, A., Meilijson, I., Gophna, U., Sharan, R., & Ruppin, E. (2010). The large-scale organization of the bacterial network of ecological co-occurrence interactions. *Nucleic Acids Res*, *38*(12), 3857-3868. https://doi.org/10.1093/nar/gkq118

Golden, A. R., Adam, H. J., Karlowsky, J. A., Baxter, M., Nichol, K. A., Martin, I., Demczuk, W., Van Caeseele, P., Gubbay, J. B., Lefebvre, B., Levett, P. N., Zahariadis, G., Haldane, D., Gad, R., German, G., Gilmour, M. W., Mulvey, M. R., Hoban, D. J., Zhanel, G. G., & Alliance, t. C. A. R. (2018). Molecular characterization of predominant Streptococcus pneumoniae serotypes causing invasive infections in Canada: the SAVE study, 2011–15. *Journal of Antimicrobial Chemotherapy*, *73*(suppl_7), vii20-vii31. https://doi.org/10.1093/jac/dky157

Gupta, N. (2019). DNA Extraction and Polymerase Chain Reaction. *J Cytol*, *36*(2), 116-117. https://doi.org/10.4103/joc.Joc_110_18

Hardie, J. M., & Whiley, R. A. (1995). The genus Streptococcus. In B. J. B. Wood & W. H. Holzapfel (Eds.), *The Genera of Lactic Acid Bacteria* (pp. 55-124). Springer US. https://doi.org/10.1007/978-1-4615-5817-0_4

Heilbronner, S., Krismer, B., Brötz-Oesterhelt, H., & Peschel, A. (2021). The microbiome-shaping roles of bacteriocins. *Nature Reviews Microbiology*, *19*(11), 726-739. https://doi.org/10.1038/s41579-021-00569-w

Janda, J. M., & Abbott, S. L. (2007). 16S rRNA gene sequencing for bacterial identification in the diagnostic laboratory: pluses, perils, and pitfalls. *J Clin Microbiol*, *45*(9), 2761-2764. https://doi.org/10.1128/jcm.01228-07

Jolley, K. A., Bray, J. E., & Maiden, M. C. J. (2018). Open-access bacterial population genomics: BIGSdb software, the PubMLST.org website and their applications. *Wellcome Open Res*, *3*, 124. https://doi.org/10.12688/wellcomeopenres.14826.1

Jones, N., Bohnsack, J. F., Takahashi, S., Oliver, K. A., Chan, M. S., Kunst, F., Glaser, P., Rusniok, C., Crook, D. W., Harding, R. M., Bisharat, N., & Spratt, B. G. (2003). Multilocus sequence typing system for group B streptococcus. *J Clin Microbiol*, *41*(6), 2530-2536. https://doi.org/10.1128/jcm.41.6.2530-2536.2003

Kerr, B., Riley, M. A., Feldman, M. W., & Bohannan, B. J. M. (2002). Local dispersal promotes biodiversity in a real-life game of rock–paper–scissors. *Nature*, *418*(6894), 171-174. https://doi.org/10.1038/nature00823

Khehra, N., Padda, I. S., & Swift, C. J. (2023). Polymerase Chain Reaction (PCR). In *StatPearls*. StatPearls Publishing

Copyright © 2023, StatPearls Publishing LLC.

Kjos, M., Miller, E., Slager, J., Lake, F. B., Gericke, O., Roberts, I. S., Rozen, D. E., & Veening, J. W. (2016). Expression of Streptococcus pneumoniae Bacteriocins Is Induced by Antibiotics via Regulatory Interplay with the Competence System. *PLoS Pathog*, *12*(2), e1005422. https://doi.org/10.1371/journal.ppat.1005422

Krzyściak, W., Pluskwa, K. K., Jurczak, A., & Kościelniak, D. (2013). The pathogenicity of the Streptococcus genus. *Eur J Clin Microbiol Infect Dis*, *32*(11), 1361-1376. https://doi.org/10.1007/s10096-013-1914-9

Kuhn, T., Mamin, M., Bindschedler, S., Bshary, R., Estoppey, A., Gonzalez, D., Palmieri, F., Junier, P., & Richter, X.-Y. L. (2022). Spatial scales of competition and a growth–motility trade-off interact to determine bacterial coexistence. *Royal Society Open Science*, *9*(12), 211592. https://doi.org/doi:10.1098/rsos.211592

Lanie, J. A., Ng, W. L., Kazmierczak, K. M., Andrzejewski, T. M., Davidsen, T. M., Wayne, K. J., Tettelin, H., Glass, J. I., & Winkler, M. E. (2007). Genome sequence of Avery's virulent serotype 2 strain D39 of Streptococcus pneumoniae and comparison with that of unencapsulated laboratory strain R6. *J Bacteriol*, *189*(1), 38-51. https://doi.org/10.1128/jb.01148-06

Mann, E. R., Bernardo, D., English, N. R., Landy, J., Al-Hassi, H. O., Peake, S. T., Man, R., Elliott, T. R., Spranger, H., Lee, G. H., Parian, A., Brant, S. R., Lazarev, M., Hart, A. L., Li, X., & Knight, S. C. (2016). Compartment-specific immunity in the human gut:

properties and functions of dendritic cells in the colon versus the ileum. *Gut*, *65*(2), 256-270. https://doi.org/10.1136/gutjnl-2014-307916
Maricic, N., & Dawid, S. (2014). Using the overlay assay to qualitatively measure bacterial production of and sensitivity to pneumococcal bacteriocins. *J Vis Exp*(91), e51876. https://doi.org/10.3791/51876
Milani, C., Duranti, S., Bottacini, F., Casey, E., Turroni, F., Mahony, J., Belzer, C., Delgado Palacio, S., Arboleya Montes, S., Mancabelli, L., Lugli, G. A., Rodriguez, J. M., Bode, L., de Vos, W., Gueimonde, M., Margolles, A., van Sinderen, D., & Ventura, M. (2017). The First Microbial Colonizers of the Human Gut: Composition, Activities, and Health Implications of the Infant Gut Microbiota. *Microbiol Mol Biol Rev*, *81*(4). https://doi.org/10.1128/mmbr.00036-17
Miller, E. L., Abrudan, M. I., Roberts, I. S., & Rozen, D. E. (2016). Diverse Ecological Strategies Are Encoded by Streptococcus pneumoniae Bacteriocin-Like Peptides. *Genome Biol Evol*, *8*(4), 1072-1090. https://doi.org/10.1093/gbe/evw055
Miller, E. L., Kjos, M., Abrudan, M. I., Roberts, I. S., Veening, J. W., & Rozen, D. E. (2018). Eavesdropping and crosstalk between secreted quorum sensing peptide signals that regulate bacteriocin production in Streptococcus pneumoniae. *Isme j*, *12*(10), 2363-2375. https://doi.org/10.1038/s41396-018-0178-x
Ogobuiro, I., Gonzales, J., Shumway, K. R., & Tuma, F. (2023). Physiology, Gastrointestinal. In *StatPearls*. StatPearls Publishing
Copyright © 2023, StatPearls Publishing LLC.
Ormaasen, I., Rudi, K., Diep, D. B., & Snipen, L. (2023). Metagenome-mining indicates an association between bacteriocin presence and strain diversity in the infant gut. *BMC Genomics*, *24*(1), 295. https://doi.org/10.1186/s12864-023-09388-0
Patterson, M. J. (1996). Streptococcus. In S. Baron (Ed.), *Medical Microbiology*. University of Texas Medical Branch at Galveston
Copyright © 1996, The University of Texas Medical Branch at Galveston.
Pianka, E. R. (1970). On r- and K-Selection. *The American Naturalist*, *104*(940), 592-597. https://doi.org/10.1086/282697
Ram, Y., Dellus-Gur, E., Bibi, M., Karkare, K., Obolski, U., Feldman, M. W., Cooper, T. F., Berman, J., & Hadany, L. (2019). Predicting microbial growth in a mixed culture from growth curve data. *Proceedings of the National Academy of Sciences of the United States of America*, *116*(29), 14698-14707. https://doi.org/10.1073/pnas.1902217116
Reading, N. C., & Sperandio, V. (2006). Quorum sensing: the many languages of bacteria. *FEMS Microbiology Letters*, *254*(1), 1-11. https://doi.org/10.1111/j.1574-6968.2005.00001.x
Reyman, M., Van Houten, M. A., Van Baarle, D., Bosch, A. A. T. M., Man, W. H., Chu, M. L. J. N., Arp, K., Watson, R. L., Sanders, E. A. M., Fuentes, S., & Bogaert, D. (2019). Impact of delivery mode-associated gut microbiota dynamics on health in the first year of life. *Nature Communications*, *10*(1). https://doi.org/10.1038/s41467-019-13014-7
Sanger, F., Nicklen, S., & Coulson, A. R. (1977). DNA sequencing with chain-terminating inhibitors. *Proceedings of the National Academy of Sciences of the United States of America*, *74*(12), 5463-5467. https://doi.org/10.1073/pnas.74.12.5463
Sievers, F., Wilm, A., Dineen, D., Gibson, T. J., Karplus, K., Li, W., Lopez, R., McWilliam, H., Remmert, M., Söding, J., Thompson, J. D., & Higgins, D. G. (2011). Fast, scalable generation of high-quality protein multiple sequence alignments using Clustal Omega. *Molecular systems biology*, *7*, 539. Retrieved 2011/10//, from http://europepmc.org/abstract/MED/21988835
https://www.ncbi.nlm.nih.gov/pmc/articles/pmid/21988835/?tool=EBI
https://www.ncbi.nlm.nih.gov/pmc/articles/pmid/21988835/pdf/?tool=EBI

https://doi.org/10.1038/msb.2011.75
https://europepmc.org/articles/PMC3261699
https://europepmc.org/articles/PMC3261699?pdf=render
Tan, S. C., & Yiap, B. C. (2009). DNA, RNA, and protein extraction: the past and the present. *J Biomed Biotechnol*, *2009*, 574398. https://doi.org/10.1155/2009/574398
Thomas, T., Gilbert, J., & Meyer, F. (2012). Metagenomics - a guide from sampling to data analysis. *Microbial Informatics and Experimentation*, *2*(1), 3. https://doi.org/10.1186/2042-5783-2-3
Tobias, A., & Sadiq, N. M. (2023). Physiology, Gastrointestinal Nervous Control. In *StatPearls*. StatPearls Publishing
Copyright © 2023, StatPearls Publishing LLC.
Totomoch-Serra, A., Marquez, M. F., & Cervantes-Barragán, D. E. (2017). Sanger sequencing as a first-line approach for molecular diagnosis of Andersen-Tawil syndrome. *F1000Res*, *6*, 1016. https://doi.org/10.12688/f1000research.11610.1
Trosvik, P., Skånseng, B., Jakobsen, K. S., Stenseth, N. C., Naes, T., & Rudi, K. (2007). Multivariate analysis of complex DNA sequence electropherograms for high-throughput quantitative analysis of mixed microbial populations. *Appl Environ Microbiol*, *73*(15), 4975-4983. https://doi.org/10.1128/aem.00128-07
Vadstein, O., Attramadal, K. J. K., Bakke, I., & Olsen, Y. (2018). K-Selection as Microbial Community Management Strategy: A Method for Improved Viability of Larvae in Aquaculture. *Front Microbiol*, *9*, 2730. https://doi.org/10.3389/fmicb.2018.02730
Weiser, J. N., Ferreira, D. M., & Paton, J. C. (2018). Streptococcus pneumoniae: transmission, colonization and invasion. *Nature Reviews Microbiology*, *16*(6), 355-367. https://doi.org/10.1038/s41579-018-0001-8
Yao, Y., Cai, X., Ye, Y., Wang, F., Chen, F., & Zheng, C. (2021). The Role of Microbiota in Infant Health: From Early Life to Adulthood [Review]. *Frontiers in Immunology*, *12*. https://doi.org/10.3389/fimmu.2021.708472

Appendices

Appendix A: Growth media

THY (500 ml)

15 g Bacto™ Todd-Hewitt Broth (BD, USA)

7.5 g Bacto™ Yeast Extract (BD, USA)

6 g Agar Powder (VWR, USA)

500 ml Milli-Q water

THY agar (500 ml)

15 g Bacto™ Todd-Hewitt Broth (BD, USA)

7.5 g Bacto™ Yeast Extract (BD, USA)

6 g Agar Powder (VWR, USA)

500 ml Milli-Q water

THY soft agar (200 ml)

6 g Bacto™ Todd-Hewitt Broth (BD, USA)

3 g Bacto™ Yeast Extract (BD, USA)

1.6 g Agar Powder (VWR, USA)

200 ml Milli-Q water

TSA (500 ml)

15 g Bacto™ Tryptic Soy Broth (BD, USA)

6 g Agar Powder (VWR, USA)

500 ml Milli-Q water

Appendix B: Gel electrophoresis

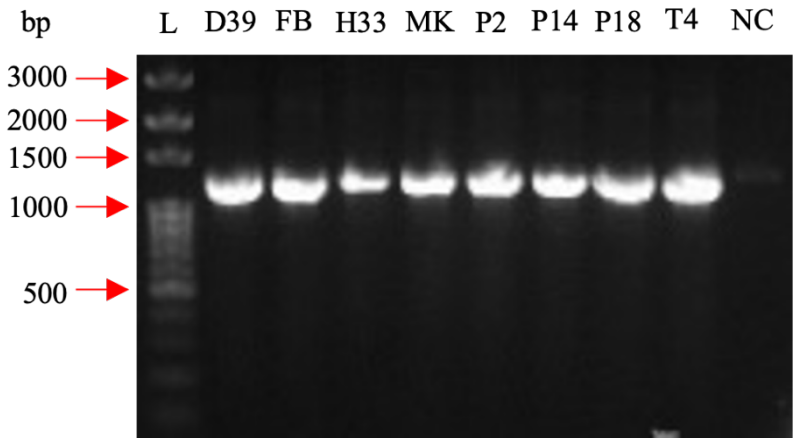

Figure B.1: Purified 16S rRNA in *S. pneumoniae* strains. The gel picture displays purified 16S rRNA in *S. pneumoniae* strains D39, FB145 (FB), Hermans-33 (H33), MK1203 (MK), PMEN-2 (P2), PMEN-14 (P14), PMEN-18 (P18), and TIGR4 (T4). 100 bp ladder (L) was used as size marker and nuclease-free water was used as negative control (NC)

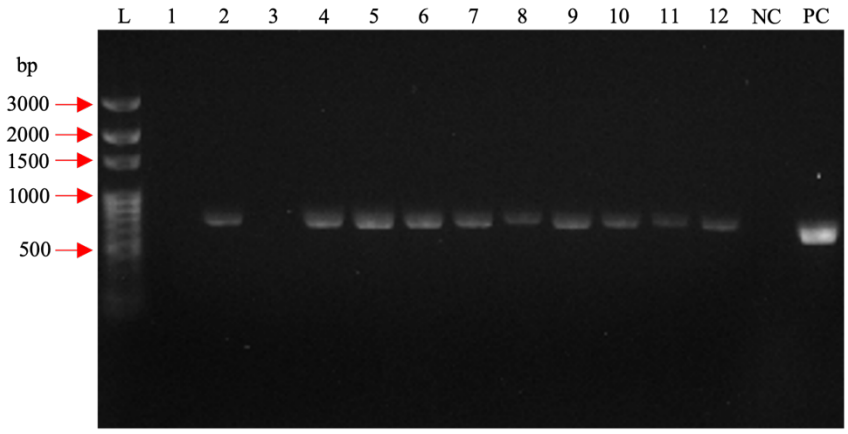

Figure B.2: Purified *gdh* in mixed cultures at 0 hours. The gel picture displays purified *gdh* in the first replicates of mixed cultures 1-12, listed in table 2.2, at 0 hours. 100 bp ladder (L) was used as size marker, nuclease-free water was used as negative control (NC), and previously purified *gdh* from pure culture of D39 was used as positive control (PC).

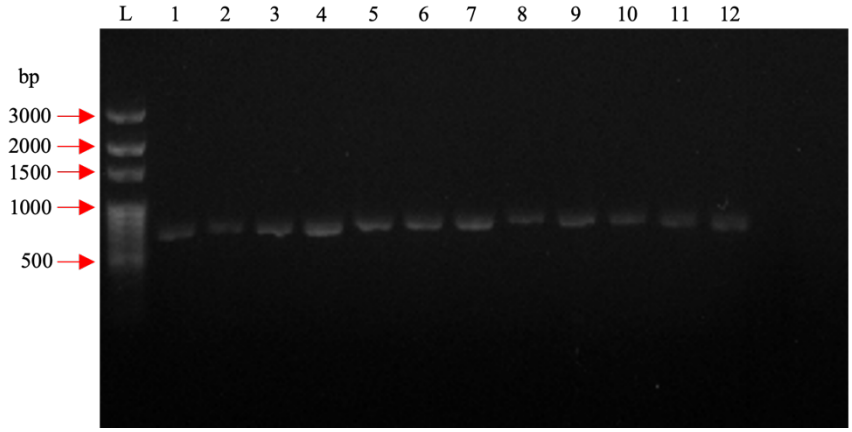

Figure B.3: Purified *gdh* in mixed cultures at 0 hours. The gel picture displays purified *gdh* in the second replicates of mixed cultures 1-12, listed in table 2.2, at 0 hours. 100 bp ladder (L) was used as size marker, and negative and positive control were loaded in the upper wells of the gel, displayed in figure B.2.

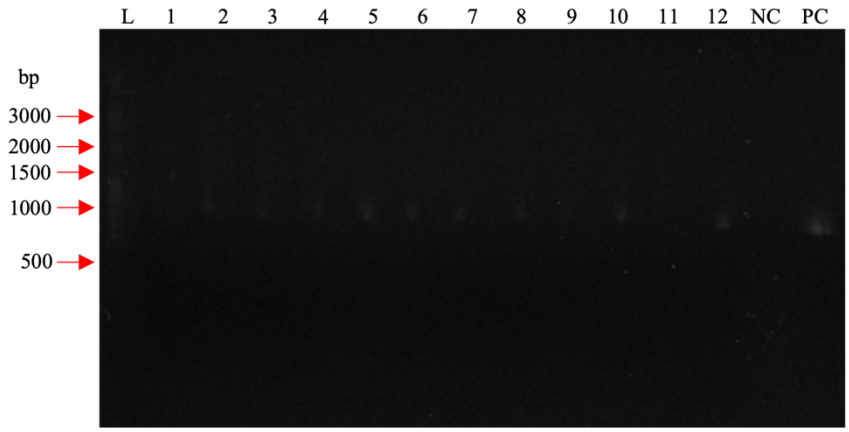

Figure B.4: Purified *gdh* in mixed cultures at 0 hours. The gel picture displays purified *gdh* in the first replicates of mixed cultures 1-12, listed in table 2.2, at 0 hours. 100 bp ladder (L) was used as size marker, nuclease-free water was used as negative control (NC), and previously purified *gdh* from pure culture of D39 was used as positive control (PC). Due to the gel being too thin, the samples are only visible as faint bands.

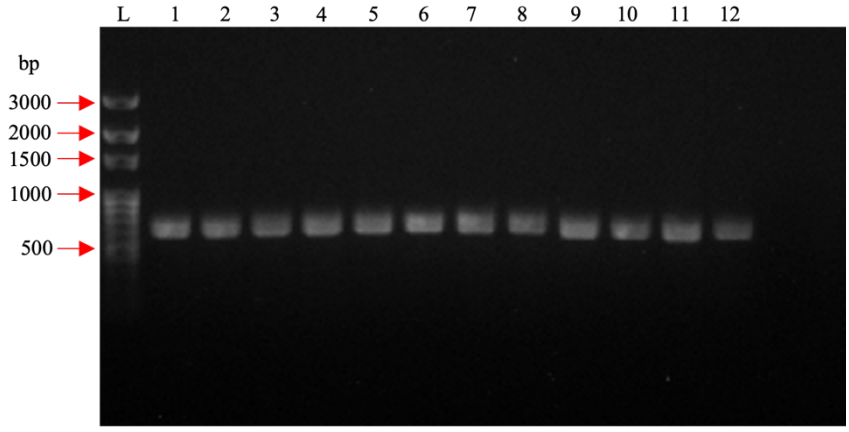

Figure B.5: Purified *gdh* in mixed cultures at 3 hours. The gel picture displays purified *gdh* in the second replicates of mixed cultures 1-12, listed in table 2.2, at 3 hours. 100 bp ladder (L) was used as size marker, and negative and positive control were loaded in the upper wells of the gel, displayed in figure B.4.

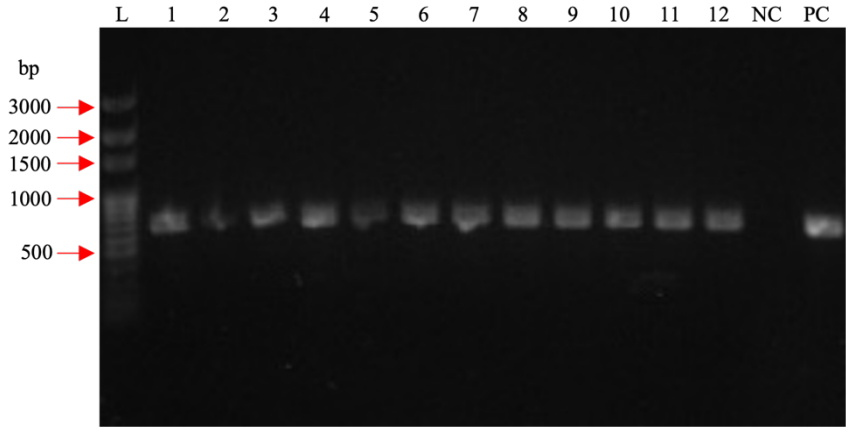

Figure B.6: Purified *gdh* in mixed cultures at 5 hours. The gel picture displays purified *gdh* in the first replicates of mixed cultures 1-12, listed in table 2.2, at 5 hours. 100 bp ladder (L) was used as size marker, nuclease-free water was used as negative control (NC), and previously purified *gdh* from pure culture of D39 was used as positive control (PC).

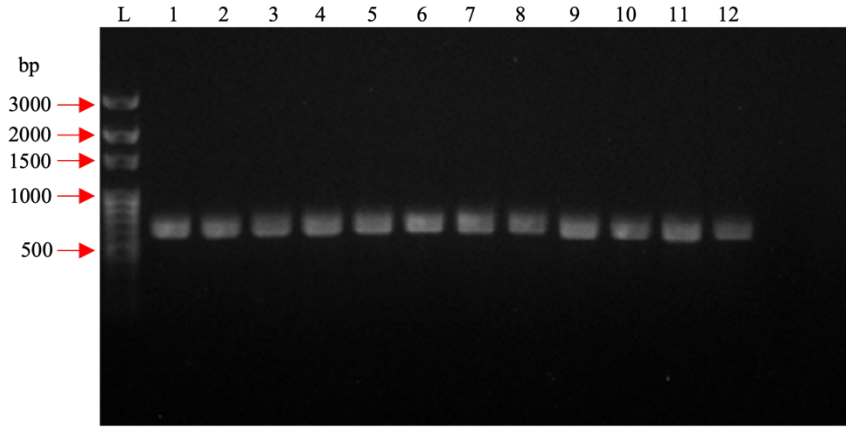

Figure B.7: Purified *gdh* in mixed cultures at 5 hours. The gel picture displays purified *gdh* in the second replicates of mixed cultures 1-12, listed in table 2.2, at 5 hours. 100 bp ladder (L) was used as size marker, and negative and positive control were loaded in the upper wells of the gel, displayed in figure B.6.

Appendix C: Polymorphic sites in *gdh*

Table C.1: Polymorphic sites in *gdh*. The table list all polymorphic sites in the housekeeping gene *gdh* identified during MLST of strains D39, Hermans-33, and PMEN-14. The nucleotides adenine (A), cytosine (C), guanine (G), and thymine (T) colored red depicts mutations from D39 as a reference.

Polymorphic site	Position (bp)	D39	Hermans-33	PMEN-14
1	26	G	A	G
2	28	G	T	G
3	31	T	C	T
4	35	A	G	A
5	41	G	G	A
6	64	A	T	C
7	89	A	A	G
8	98	G	A	G
9	106	G	A	G
10	125	T	C	C
11	155	A	G	A
12	161	A	A	G
13	170	G	G	A
14	176	A	C	A
15	191	C	T	C
16	230	A	G	A
17	239	G	A	G
18	254	A	G	A
19	272	A	G	A
20	290	T	A	T
21	302	A	G	A
22	323	G	A	G
23	343	C	T	C
24	344	A	G	A
25	350	T	A	T
26	359	T	A	T
27	368	A	G	A
28	410	G	A	G
29	421	T	C	T
30	437	T	A	T
31	473	C	C	T
32	503	G	A	G
33	512	G	A	G
34	521	C	A	C
35	533	G	A	G
36	536	T	C	T
37	556	A	G	A
38	563	T	C	T
39	581	T	C	T

Appendix D: Hemolysis on TSA+SB plates

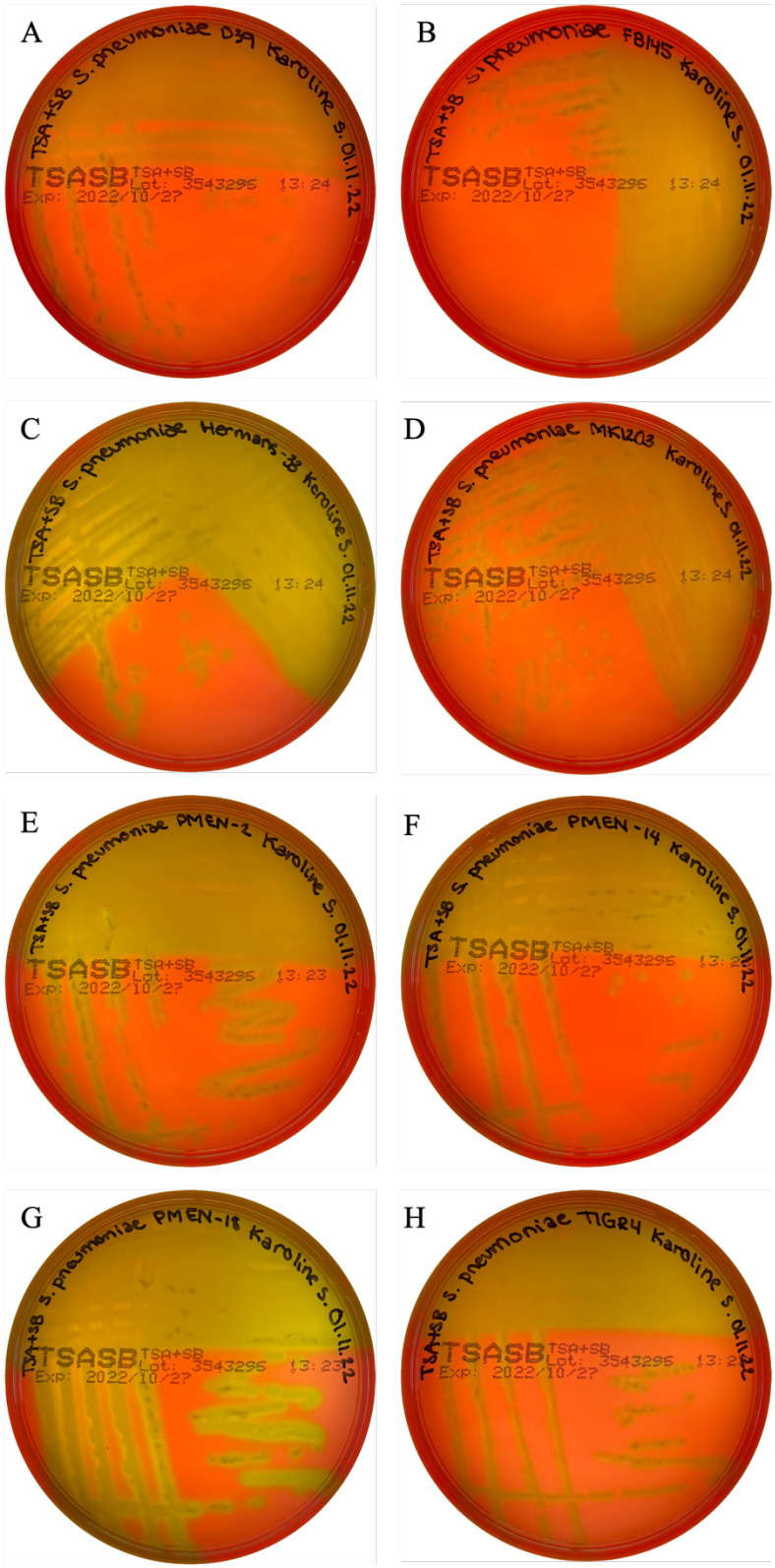

Figure D.1: Hemolysis on TSA+SB plates. The images reveal α-hemolysis on TSA+SB plates by *S. pneumoniae* strains (A) D39, (B) FB145, (C) Hermans-33, (D) MK1203, (E) PMEN-2, (F) PMEN-14, (G) PMEN-18, and (H) TIGR4 after O/N incubation at 37°C with 5 % CO_2.

Appendix E: Overlay assays after competition on plate

Table E.1: Inhibition zones generated by producer strains cultured on THY in the first round of competition on plate. The table presents the diameter of the inhibition zones in mm created by each producer strain initially cultured on THY agar, listed vertically, during the first round of competition on plate. Horizontally, the overlay strains are listed from D39, to FB145 (FB), Hermans-33 (H33), MK1203 (MK), PMEN-2 (P2), PMEN-14 (P14), PMEN-18 (P18), and TIGR4 (T4). PMEN-14 did not grow in the overlay, hence N/A.

Producer strain	D39	FB	H33	MK	P2	P14	P18	T4	Mean
D39	3	1	0	0	1	N/A	0	0	0.7
FB145	3	1	0	3	5	N/A	2	0	2.0
Hermans-33	6.5	3	2	6.5	6.5	N/A	6	6	5.2
MK1203	0	1	0	3	0	N/A	0	0	0.6
PMEN-2	0	1	0	0	2	N/A	0	2	0.7
PMEN-14	0	0	0	0	2	N/A	0	0	0.3
PMEN-18	3	3	2	3	6	N/A	2	4	3.3
TIGR4	3	2	1	3	5	N/A	0	4	2.6

Table E.2: Inhibition zones generated by producer strains cultured on TSA+SB in the first round of competition on plate. The table presents the diameter of the inhibition zones in mm created by each producer strain initially cultured on TSA+SB, listed vertically, during the first round of competition on plate. Horizontally, the overlay strains are listed from D39, to FB145 (FB), Hermans-33 (H33), MK1203 (MK), PMEN-2 (P2), PMEN-14 (P14), PMEN-18 (P18), and TIGR4 (T4). PMEN-14 did not grow in the overlay, hence N/A.

Producer strain	D39	FB	H33	MK	P2	P14	P18	T4	Mean
D39	3	3	0	3	5	N/A	4	2	2.9
FB145	4	3	0	4	5	N/A	3	3	3.1
Hermans-33	7	7	2	7	7.5	N/A	7	6	6.2
MK1203	4.5	3	0	2	6	N/A	0	0	2.2
PMEN-2	2	1	1	3	3	N/A	0	2	1.7
PMEN-14	3	2	0	3	4	N/A	0	2	2.0
PMEN-18	4	3	2	3	5	N/A	2	3	3.1
TIGR4	4	3	1	3	5	N/A	0	6	3.1

Table E.3: Inhibition zones generated by producer strains cultured on TSA+SB in the second round of competition on plate. The table presents the diameter of the inhibition zones in mm created by each producer initially strain cultured on TSA+SB, listed vertically, during the second round of competition on plate. Horizontally, the overlay strains are listed from D39, to FB145 (FB), Hermans-33 (H33), MK1203 (MK), PMEN-2 (P2), PMEN-14 (P14), PMEN-18 (P18), and TIGR4 (T4).

Producer strain	D39	FB	H33	MK	P2	P14	P18	T4	Mean
D39	4	4	0	5.5	6	3	1	2	3.2
FB145	5	3.5	0	5.5	5.5	4	0	2	3.2
Hermans-33	6.5	6.5	0	6	5	6	5	6	5.1
MK1203	5	3	0	3.5	3	0	0	3	2.2
PMEN-2	3	4	0	5	5.5	1	0	2	2.6
PMEN-14	4	4	0	4.5	6	3	1	2	3.1
PMEN-18	6	4	0	4.5	6	2	1	3	3.3
TIGR4	6.5	5	0	4.5	6	0	0	4	3.3

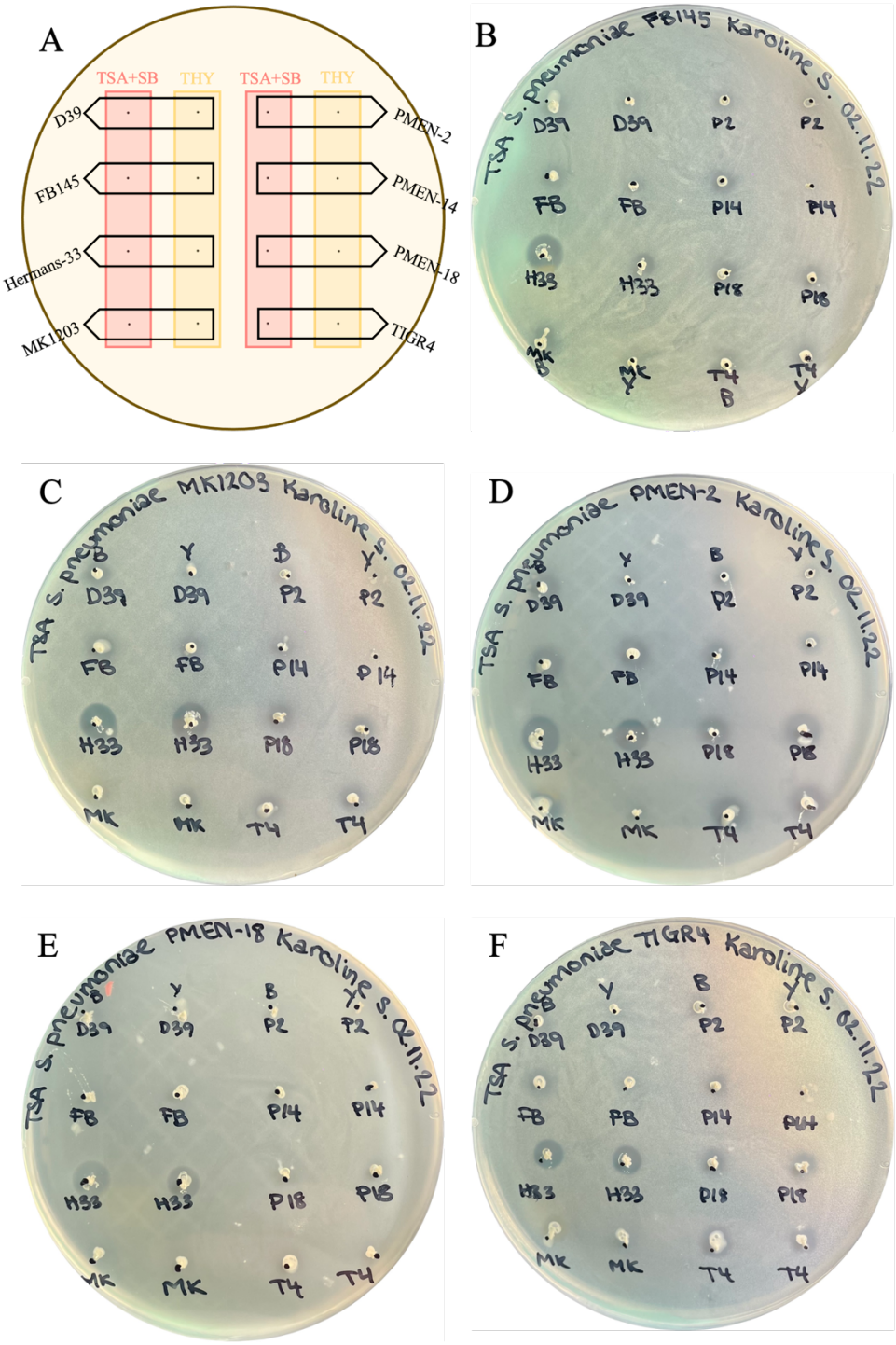

Figure E.1: Overlay assays after first round of competition on plate. The figure displays (A) illustration of how each plate was stabbed with each producer strain two times, one initially cultured on THY agar and the other on TSA+SB, followed by results from the first round of competition on plate with (B) FB145, (C) MK1203, and (D) PMEN-2, (E) PMEN-18, and (F) TIGR4 as the overlay strain.

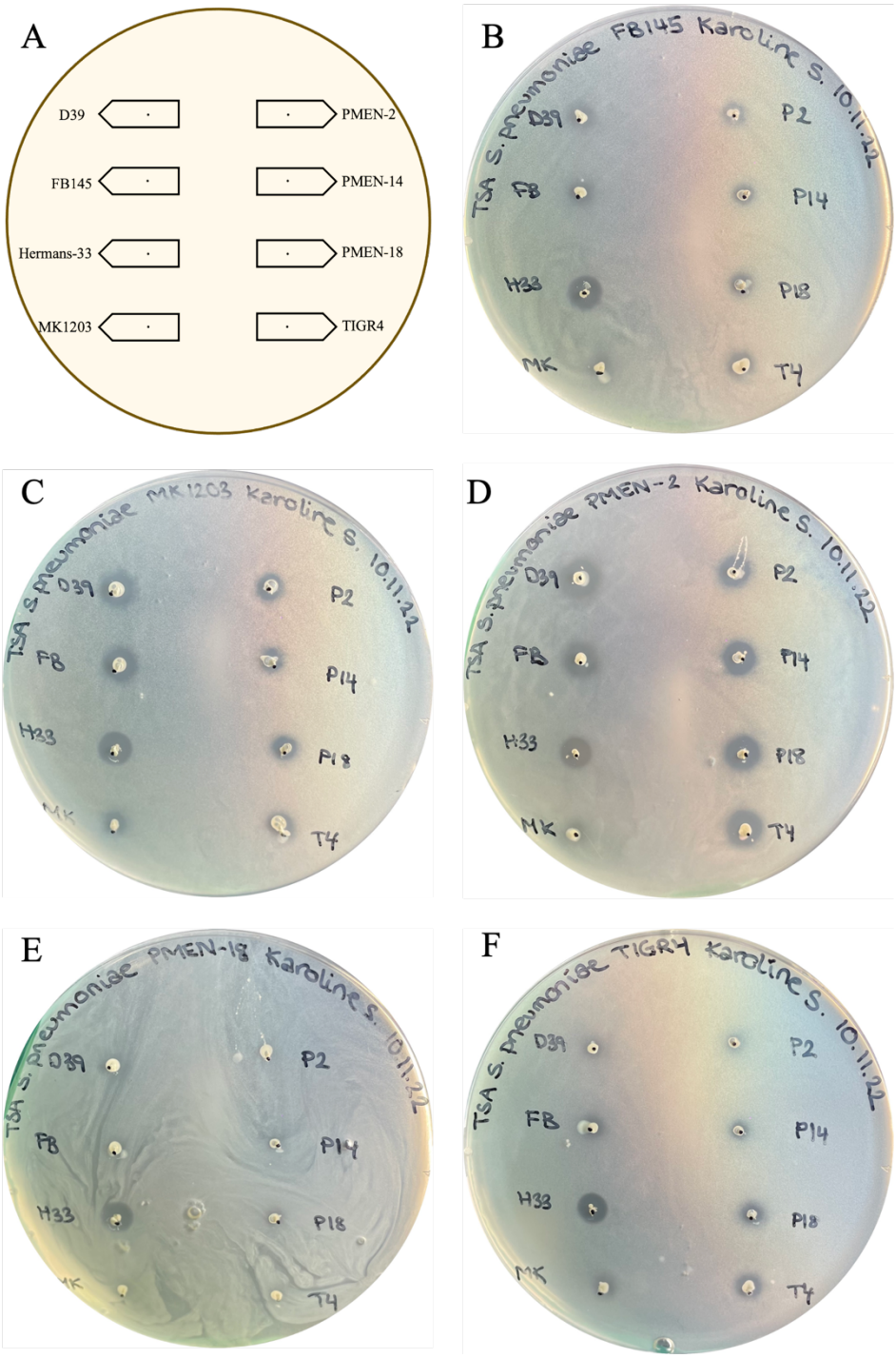

Figure E.2: Overlay assays after second round of competition on plate. The figure displays (A) illustration of how each plate was stabbed with each producer strain initially cultured on TSA+SB, followed by results from the first round of competition on plate with (B) FB145, (C) MK1203, and (D) PMEN-2, (E) PMEN-18, and (F) TIGR4 as the overlay strain.

Appendix F: Relative abundance of strains during competition in broth

Table F.1: Approximate mean relative abundance of strains during competition in broth. The table presents the approximate mean relative abundance on a scale from 0 to 1 of strains D39, Hermans-33 (H33), and PMEN-14 (P14) in the mixed cultures at 0, 3, and 5 hours into the competition in broth. At 0 hours, some samples generated sequences of low quality yielding non-interpretable results, hence N/A.

Replicate	Strain 1, agar	0 hours	3 hours	5 hours	Strain 2, agar	0 hours	3 hours	5 hours
1	D39, TSA+SB	N/A	0.75	1	H33, TSA+SB	N/A	0.25	0
2	D39, TSA+SB	0.75	0.75	1	H33, TSA+SB	0.25	0.25	0
1	D39, TSA+SB	0.75	0.75	1	H33, THY	0.25	0.25	0
2	D39, TSA+SB	0.75	0.75	1	H33, THY	0.25	0.25	0
1	D39, THY	0.75	0.75	1	H33, THY	0.25	0.25	0
2	D39, THY	N/A	0.75	1	H33, THY	N/A	0.25	0
1	D39, THY	0.5	1	1	H33, TSA+SB	0.5	0	0
2	D39, THY	0.75	1	1	H33, TSA+SB	0.25	0	0
1	D39, TSA+SB	N/A	0.5	0.25	P14, TSA+SB	N/A	0.5	0.75
2	D39, TSA+SB	0.75	0.5	0.25	P14, TSA+SB	0.25	0.5	0.75
1	D39, TSA+SB	0.25	0.25	0.25	P14, THY	0.75	0.75	0.75
2	D39, TSA+SB	N/A	0.25	0.25	P14, THY	N/A	0.75	0.75
1	D39, THY	0.25	0.25	0.25	P14, THY	0.75	0.75	0.75
2	D39, THY	N/A	0.25	0.25	P14, THY	N/A	0.75	0.75
1	D39, THY	N/A	0.25	0.5	P14, TSA+SB	N/A	0.75	0.5
2	D39, THY	0.75	0.5	0.75	P14, TSA+SB	0.25	0.5	0.25
1	H33, TSA+SB	N/A	0.25	0	P14, TSA+SB	N/A	0.75	1
2	H33, TSA+SB	0.5	0	0	P14, TSA+SB	0.5	1	1
1	H33, TSA+SB	0.5	0	0	P14, THY	0.5	1	1
2	H33, TSA+SB	0.5	0	0	P14, THY	0.5	1	1
1	H33, THY	0.5	0	0	P14, THY	0.5	1	1
2	H33, THY	N/A	0	0	P14, THY	N/A	1	1
1	H33, THY	0.75	0	0	P14, TSA+SB	0.25	1	1
2	H33, THY	0.5	0.25	0	P14, TSA+SB	0.5	0.75	1

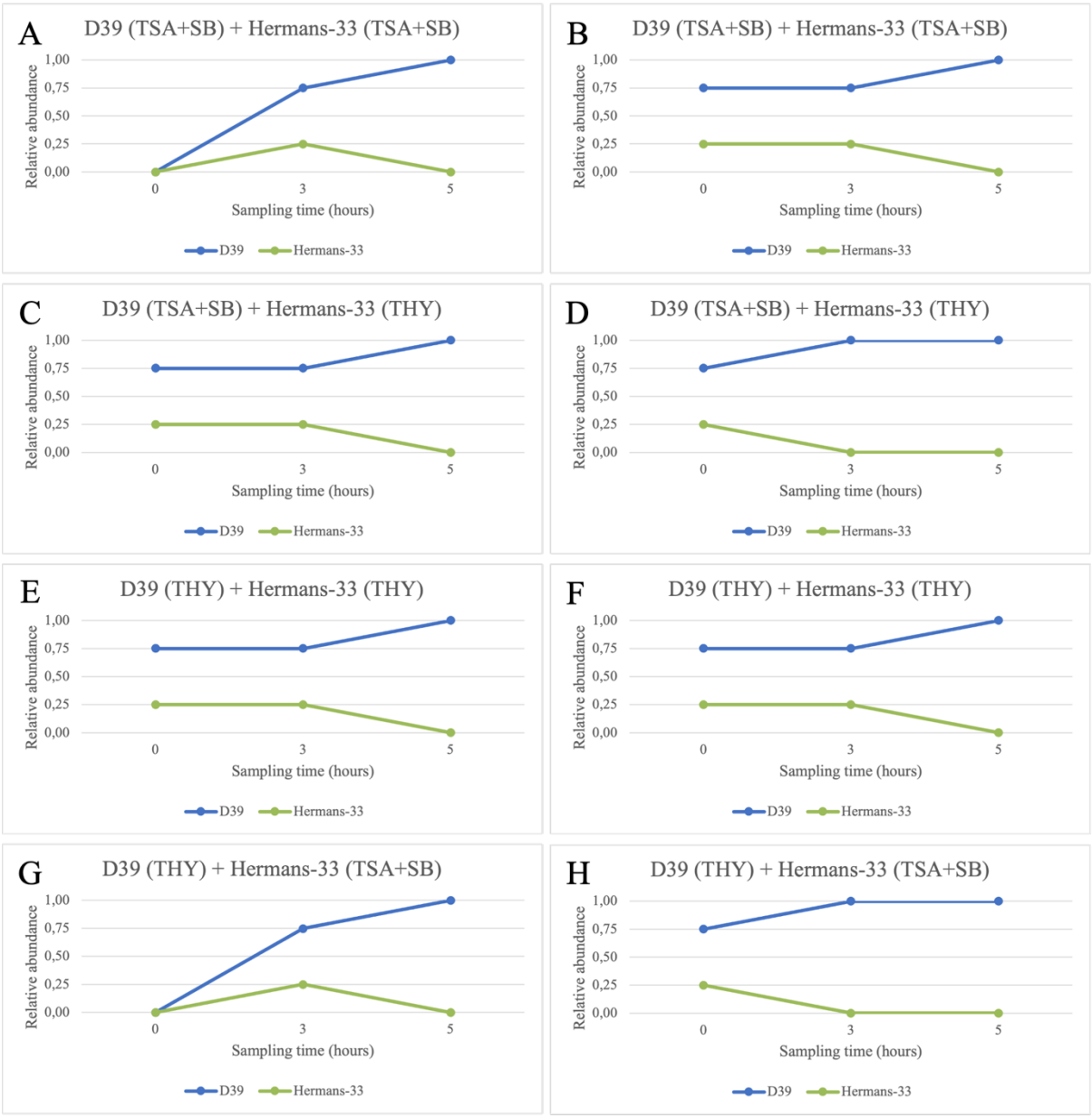

Figure F.1: Relative abundance of D39 and Hermans-33 during competition in broth. The graphs illustrate the relative abundance of D39, depicted in blue, and Hermans-33, depicted in green, on a scale from 0 to 1 in each mixed strain sample at 0, 3, and 5 hours into the competition in broth. Strains were mixed in four possible ways and replicates were sampled at each time point, with (A) and (B) representing D39 cultured on TSA+SB mixed with Hermans-33 cultured on TSA+SB, (C) and (D) representing D39 cultured on TSA+SB and Hermans-33 cultured on THY, (E) and (F) representing D39 cultured on THY mixed with Hermans-33 cultured on THY, and (G) and (H) representing D39 cultured on THY mixed with Hermans-33 cultured on TSA+SB.

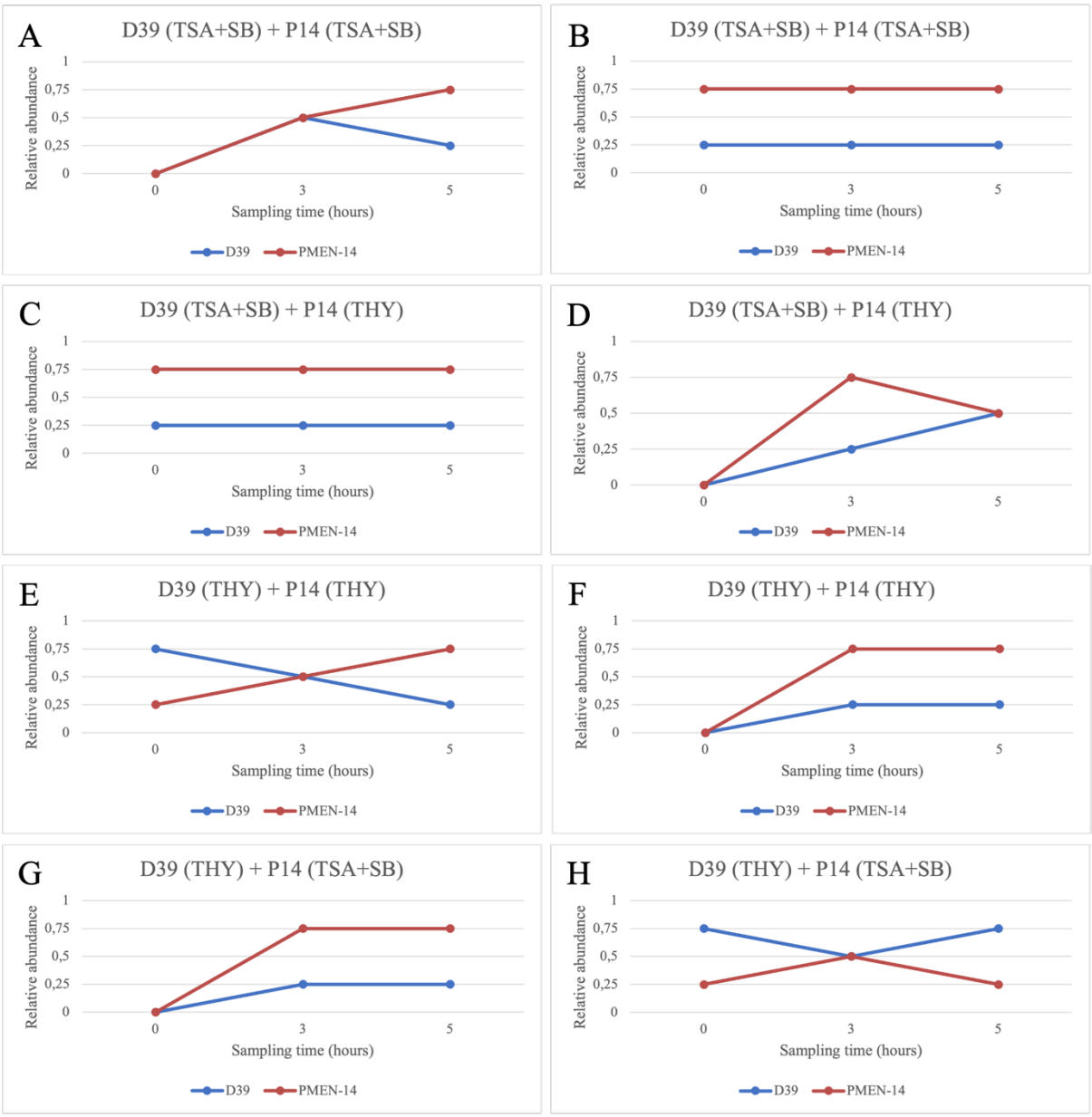

Figure F.2: Relative abundance of D39 and PMEN-14 during competition in broth. The graphs illustrate the relative abundance of D39, depicted in blue, and PMEN-14, depicted in red, on a scale from 0 to 1 in each mixed strain sample at 0, 3, and 5 hours into the competition in broth. Strains were mixed in four possible ways and replicates were sampled at each time point, with (A) and (B) representing D39 cultured on TSA+SB mixed with PMEN-14 cultured on TSA+SB, (C) and (D) representing D39 cultured on TSA+SB and PMEN-14 cultured on THY, (E) and (F) representing D39 cultured on THY mixed with PMEN-14 cultured on THY, and (G) and (H) representing D39 cultured on THY mixed with PMEN-14 cultured on TSA+SB.

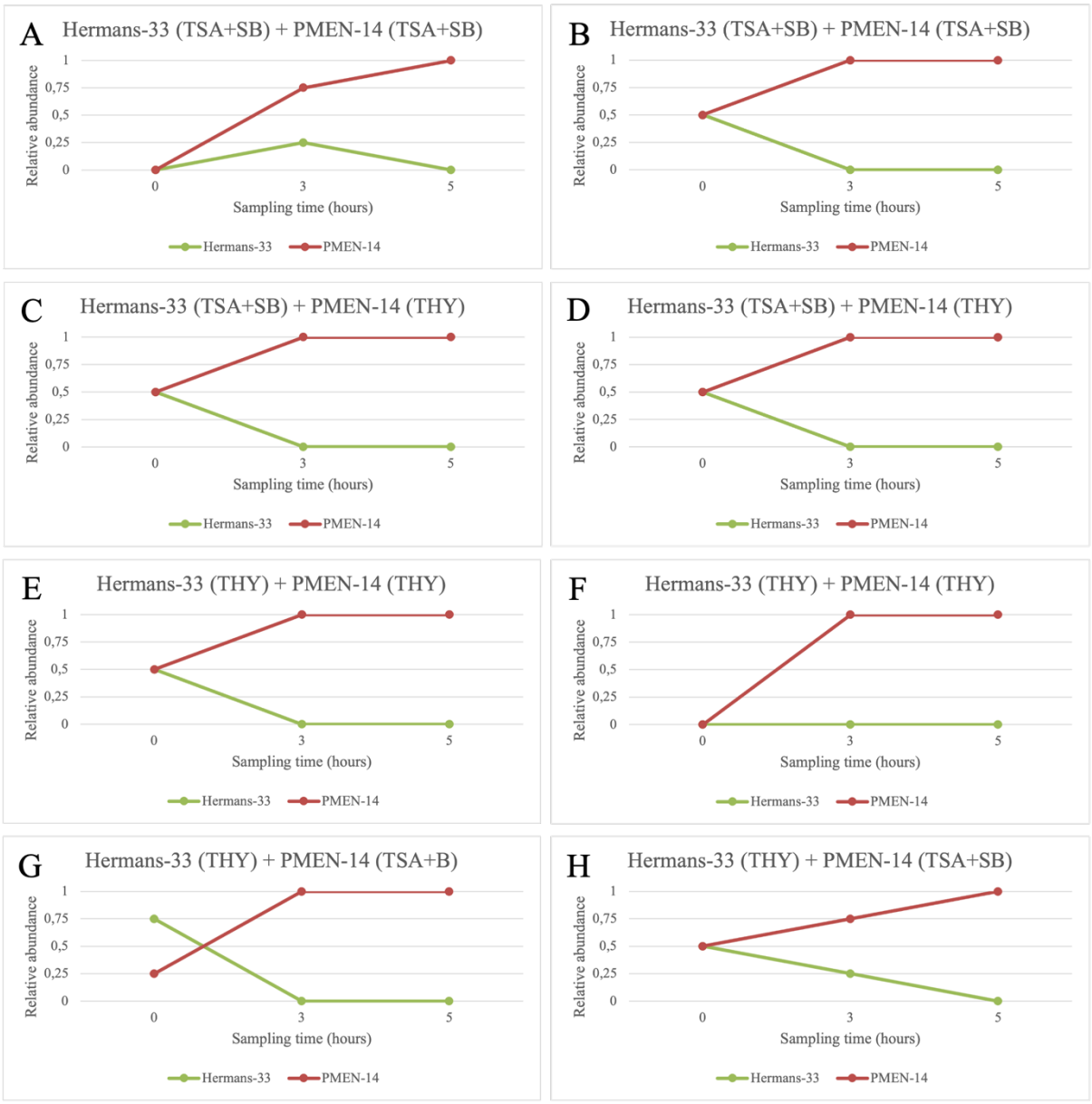

Figure F.3: Relative abundance of Hermans-33 and PMEN-14 during competition in broth. The graphs illustrate the relative abundance of Hermans-33, depicted in green, and PMEN-14, depicted in red, on a scale from 0 to 1 in each mixed strain sample at 0, 3, and 5 hours into the competition in broth. Strains were mixed in four possible ways and replicates were sampled at each time point, with (A) and (B) representing Hermans-33 cultured on TSA+SB mixed with PMEN-14 cultured on TSA+SB, (C) and (D) representing Hermans-33 cultured on TSA+SB and PMEN-14 cultured on THY, (E) and (F) representing Hermans-33 cultured on THY mixed with PMEN-14 cultured on THY, and (G) and (H) representing Hermans-33 cultured on THY mixed with PMEN-14 cultured on TSA+SB.

Norges miljø- og biovitenskapelige universitet
Noregs miljø- og biovitskapelege universitet
Norwegian University of Life Sciences

Postboks 5003
NO-1432 Ås
Norway